Biochimica et Biophysica Acta 1828 (2013) 2778–2792

Contents lists available at ScienceDirect

Biochimica et Biophysica Acta

journal homepage: www.elsevier.com/locate/bbamem

Review

The structure and regulation of magnesium selective ion channels

Jian Payandeh [a,*], Roland Pfoh [b], Emil F. Pai [b,c,d,e,**]

[a] Department of Structural Biology, Genentech Inc., 1 DNA Way, South San Francisco, CA 94080, USA
[b] Department of Biochemistry, University of Toronto, 1 King's College Circle, Toronto, Ontario M5S 1, Canada
[c] Department of Medical Biophysics, University of Toronto, 101 College Street, Toronto, Ontario M5G 1L7, Canada
[d] Department of Molecular Genetics, University of Toronto, 1 King's College Circle, Toronto, Ontario M5S 1A8, Canada
[e] Campbell Family Institute for Cancer Research, Ontario Cancer Institute University Health Network, 101 College Street, Toronto, Ontario M5G 1L7, Canada

ARTICLE INFO

Article history:
Received 6 May 2013
Received in revised form 30 July 2013
Accepted 2 August 2013
Available online 15 August 2013

Keywords:
Magnesium
Ion channel
Selectivity
Gating
MgtE
CorA

ABSTRACT

The magnesium ion (Mg^{2+}) is the most abundant divalent cation within cells. In man, Mg^{2+}-deficiency is associated with diseases affecting the heart, muscle, bone, immune, and nervous systems. Despite its impact on human health, little is known about the molecular mechanisms that regulate magnesium transport and storage. Complete structural information on eukaryotic Mg^{2+}-transport proteins is currently lacking due to associated technical challenges. The prokaryotic MgtE and CorA magnesium transport systems have recently succumbed to structure determination by X-ray crystallography, providing first views of these ubiquitous and essential Mg^{2+}-channels. MgtE and CorA are unique among known membrane protein structures, each revealing a novel protein fold containing distinct arrangements of ten transmembrane-spanning α-helices. Structural and functional analyses have established that Mg^{2+}-selectivity in MgtE and CorA occurs through distinct mechanisms. Conserved acidic side-chains appear to form the selectivity filter in MgtE, whereas conserved asparagines coordinate hydrated Mg^{2+}-ions within the selectivity filter of CorA. Common structural themes have also emerged whereby MgtE and CorA sense and respond to physiologically relevant, intracellular Mg^{2+}-levels through dedicated regulatory domains. Within these domains, multiple primary and secondary Mg^{2+}-binding sites serve to staple these ion channels into their respective closed conformations, implying that Mg^{2+}-transport is well guarded and very tightly regulated. The MgtE and CorA proteins represent valuable structural templates to better understand the related eukaryotic SLC41 and Mrs2–Alr1 magnesium channels. Herein, we review the structure, function and regulation of MgtE and CorA and consider these unique proteins within the expanding universe of ion channel and transporter structural biology.

Contents

* Corresponding author at: Department of Structural Biology, Genentech Inc., 1 DNA Way, South San Francisco, CA 94080, USA. Tel.: +1 650 225 6416; fax: +1 650 225 3734.
** Corresponding author at: Ontario Cancer Institute, Campbell Family Institute for Cancer Research, 101 College Street, TMDT 5-358, Toronto, Ontario M5G 1L7, Canada. Tel./fax: +1 416 581 7545.
E-mail addresses: payandeh.jian@gene.com (J. Payandeh), pai@hera.med.utoronto.ca (E.F. Pai).

0005-2736/$ – see front matter © 2013 Elsevier B.V. All rights reserved.
http://dx.doi.org/10.1016/j.bbamem.2013.08.002

1. Introduction

It is important to recognize that the chemistry and coordination geometry of the Mg^{2+} ion are unique. Mg^{2+} has the smallest ionic radius and the largest effective hydrated radius compared to the other common biological cations [1]. The Mg^{2+} ion is almost invariably hexacoordinated and maintains strict bond lengths and bond angles (2.15 Å ± 0.1 Å and 90°, respectively) [1–3]. By contrast, the coordination schemes of Na^+, K^+ and Ca^{2+} are less restrictive and more promiscuous [2–4]. As should be expected for a small, charge-dense ion, the first hydration shell of Mg^{2+} is held very tightly [1]. This distinctive chemistry undoubtedly underlies the special roles of Mg^{2+} in catalysis, biological structure, and the regulation of diverse physiological processes. Not surprisingly, the proteins which facilitate selective Mg^{2+} transport have long been thought to represent a unique class of membrane transport proteins [5–7].

Mg^{2+} is the most abundant intracellular divalent cation and an important co-factor in the machineries that replicate, transcribe and translate genomic information [8–11]. This underscores the early exploitation of Mg^{2+} during molecular evolution. As a structural co-factor, Mg^{2+} stabilizes the ribosome, lipid membranes, and nucleic acids [8,10–12]. Mg^{2+} further serves as a pivotal component in metabolic networks and signaling cascades where it participates in regulating enzyme activity and targeting macromolecules to specific complexes or cellular locations. Less appreciated roles for Mg^{2+} include competition with Ca^{2+} for key intracellular binding sites [13–16] and the regulation of virulence programs in pathogenic bacteria [17–20]. The maintenance of proper Mg^{2+} homeostasis has been correlated with physiological well being in humans. For example, Mg^{2+} deficiency is associated with pathological states including cardiac syndromes, epilepsy, migraines, muscular dysfunction and bone wasting [6,21]. Entering through the MagT1 channel, Mg^{2+} has also been identified as a key intracellular signaling molecule during immune cell activation [22].

The total intracellular Mg^{2+} content in most cell types is ~20 mM [1,23]. The free Mg^{2+} concentration is typically in the range of 0.5–1.0 mM and a considerable proportion of the complexed Mg^{2+} pool is bound as Mg^{2+}-ATP [1,23]. It has been postulated that fluctuating intracellular and extracellular magnesium concentrations should be regarded as physiologically relevant [24,25], but experimental validation of this hypothesis has been impeded by the lack of suitable methods to track changes of magnesium within a biological context. We anticipate that the development of improved magnesium probes [26] will be spawned by further identification and characterization of defects in Mg^{2+} transport systems, which lead to pathological states in humans (Table 1) [27–29]. Despite the prevalence of Mg^{2+} in biology, relatively little is known about the mechanisms regulating Mg^{2+} transport, homeostasis and storage [6,21,30].

Cellular Mg^{2+} transport systems were first identified over forty years ago [31–35]. In fact, many of these transport systems now are known to be conserved from bacteria to man (Table 1) [6,7,36]. While

Table 1
Summary of known Mg^{2+} transport systems.

Protein	Source	Membrane	TMs	Oligomeric state	Mechanism	Disease association
CorA	Prokaryotic	Plasma	10	(2 TMs × 5)	Channel	Virulence
MgtA/B	Prokaryotic	Plasma	10		P-type ATPase	Virulence
MgtC	Prokaryotic	Plasma				Virulence
MgtE	Prokaryotic	Plasma	10	(5 TMs × 2)	Channel	Virulence
MHX[a]	Plants	Vacuole	11		Exchanger	
XNTA[a]	Protozoan	Plasma	11		Channel	
ACDP	Eukaryotic	Plasma	4		Channel	UFS
Alr1/2	Eukaryotic	Plasma	10	(2 TMs × 5)	Channel	
HIP14	Eukaryotic	Golgi	6		Chanzyme[b]	Huntington
Lep10/Mrs2	Eukaryotic	Mitochondria	10	(2 TMs × 5)	Channel	MDR
MagC1	Eukaryotic					
MagT1	Eukaryotic	Plasma	4		Channel	
MMgT	Eukaryotic	Golgi	2		Channel	
Mnr2	Eukaryotic	Vacuole	10	(2 TMs × 5)		
NIPA	Eukaryotic	Plasma/endosomes	8–9	dimer	Channel	HSP
PCLN1/claudin	Eukaryotic	Tight junction	4	oligomer	Channel	HHN
SLC1-A1	Eukaryotic	Plasma	11	pseudodimer	Exchanger?	
TRPM6	Eukaryotic	Plasma	24	(6 TMs × 4)	Chanzyme[b]	HSH
TRPM7	Eukaryotic	Plasma	24	(6 TMs × 4)	Chanzyme[b]	ALS, PD

ALS, amyotrophic lateral sclerosis; HHN, hypomagnesemia with hypercalciuria and nephrocalcinosis; HSH, hypomagnesemia with hypocalcemia; HSP, hereditary spastic paraplegia; MDR, multi-drug resistance; PD, parkinsonism dementia; UFS, urofacial syndrome.

[a] Related to Na^+/Ca^{2+} exchanger.

[b] These channels also have an integral enzyme activity.

the sequence identity across evolutionarily related Mg^{2+} transport proteins tends to be low, essential amino acid motifs are highly conserved and we can anticipate many functional and structural parallels. In addition to these ubiquitous systems, several apparently unique Mg^{2+} transport proteins have also evolved within the prokaryotic and eukaryotic domains of life (Table 1) [6,7,30]. Based on the available amino acid sequences and predicted membrane topologies of these proteins, it seems likely that nature has evolved multiple structural scaffolds to selectively transport Mg^{2+} into and out of cells. This striking scenario stands in contrast to the single pore architecture that is known to define all highly selective K^+ channels [37].

To date, MgtE and CorA represent the only two Mg^{2+} transport systems which have had their complete structures determined by X-ray crystallography [38–45]. These recent advances have shed first light on the structural basis of Mg^{2+} transport and homeostasis, and have broader implications because MgtE and CorA are the prokaryotic homologues of the eukaryotic SLC41 and Mrs2–Alr1 Mg^{2+} channels, respectively. The structures of MgtE and CorA have each revealed completely distinct transmembrane (TM) topologies and yet potentially common mechanisms of Mg^{2+}-based regulation. On-going efforts to further characterize MgtE and CorA have set the stage to better understand the structural basis of regulated Mg^{2+} transport in these two wide-spread and ubiquitous systems [39,46–50]. Here, we will review the structure, function and regulation of MgtE and CorA. We will also discuss the common themes that have emerged from structural studies of other channel and transporter systems.

2. MgtE

2.1. Distribution of the MgtE system

Maguire and coworkers first identified *mgtE* in a broad range of Gram-negative and Gram-positive bacteria using classic genetic methods [51,52]. Clues to the importance of MgtE arose with the identification of *mgtE* as a potential virulence gene in *Borrelia burgdorferi*, the causative agent of Lyme disease [53]. MgtE has since been implicated in the proper functioning of the electron transport chain [54], promoting the adherence of *Aeromonas hydrophila* to human cells [55], and modulation of the Type III secretion (TSIII) machinery in *Salmonella* [56]. Notably, the Mg^{2+} transport function of MgtE was found to be dispensable for its role in TSIII regulation [56], suggesting a complex interplay between MgtE and other cellular components. These data highlight a crucial role for MgtE in bacterial physiology and pathogenesis. From recent genomic sequencing efforts, *mgtE* is now known to be present in ~50% of all prokaryotic species, where it is generally thought to function as the primary microbial Mg^{2+} transport system [57].

In eukaryotes, three *mgtE*-like genes belonging to the SLC41 family of solute carriers have been identified. Electrophysiological studies have characterized Mg^{2+}-based currents through all three SLC41 proteins but the precise physiological roles of these channels remain unclear [6,58–61]. SLC41-A1 is found in most human tissues and its expression levels are regulated by dietary Mg^{2+} uptake [6,59,62]. As found for other channel and transporter families like FocA [63] and ClC [64], the SLC41 proteins have undergone an apparent gene duplication and fusion event from their primordial *mgtE* ancestor. However, the N-terminal regulatory domains of MgtE (discussed below) are missing in the SLC41 channels, suggesting that these proteins have evolved alternate mechanisms of regulation. In fact, the distinct cytosolic N-terminal domain of SLC41-A1 appears to be required for an endosomal recycling mechanism thought to be involved in SLC41-A1 regulation [65]. Like SCL41-A1 and SCL41-A2, bacterial MgtE proteins can rescue cell growth and proliferation of TRPM7-deficient vertebrate B-cells [60]. Nevertheless, in spite of their previously reported channel-like properties, a recent study has characterized the human SLC41-A1 protein as a plasma membrane Na^+/Mg^{2+} exchanger [66]. Despite these differences, we believe studies on the related bacterial MgtE proteins will provide valuable insight into the structure, function and regulation of the SLC41 protein family.

2.2. Structure determination of MgtE

Nureki and coworkers determined the first crystal structure of MgtE from *Thermus thermophilus* in the presence of Mg^{2+} at 3.5 Å resolution [38] and later refined their model against 2.9 Å resolution data [39]. As anticipated before structure determination, MgtE presented a novel membrane protein architecture. MgtE was revealed to be a homodimer containing a large intracellular N-terminal regulatory region linked to a C-terminal membrane-embedded ion pore (Fig. 1). Mg^{2+} ions bound to the intracellular domain serve to maintain the TM ion pore in an occluded state (Fig. 1B), suggesting this represents a closed conformation of the ion channel. Crystal structures have also been determined for the soluble intracellular portion of MgtE from *T. thermophilus* [38], *Enterococcus faecalis* [67] and *Shewanella oneidensis* (PDB ID: 3KXR). These additional crystal structures have aided in the identification of Mg^{2+} binding sites and the elucidation of the potential dynamics of MgtE gating [38,39,46].

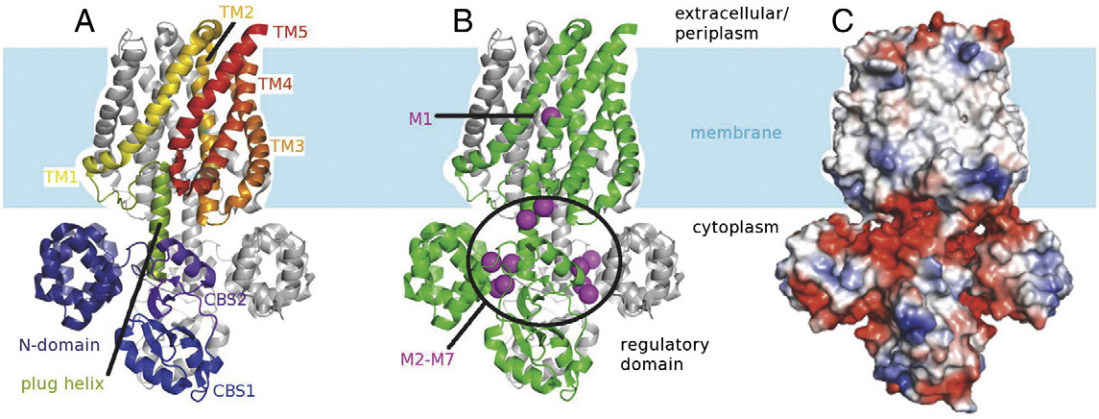

Fig. 1. Overall structure of the *Thermus thermophilus* MgtE Mg^{2+} channel in a closed state. (A) In one subunit of the MgtE dimer different colors indicate the various structural domains: N-domain (deep blue), CBS1 domain (blue), CBS2 domain (purple), plug helix (green) and trans-membrane (TM) domain (yellow-to-red gradient). (B) Thirteen Mg^{2+} ions bound in the MgtE structure are highlighted in magenta. Twelve ions are bound within and between domains of the intracellular assembly. One Mg^{2+} ion (M1) is bound in the central ion conduction pore. (C) Electrostatic surface features of MgtE with red representing acidic regions and blue representing basic regions. Note the concentration of acidic residues within the intracellular regulatory domain and their overlap with the Mg^{2+}-binding sites.

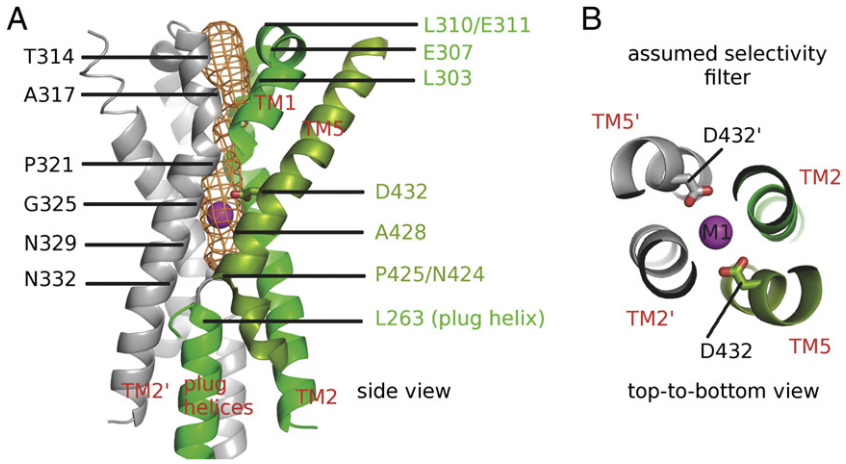

Fig. 2. Structure of the MgtE ion pore. (A) The solvent accessible pore volume calculated by MOLE [165] is rendered as an orange mesh. Only pore-forming helices are shown for clarity; pore-lining residues are indicated by black lines. Protomer A is colored green, whereas protomer B is colored gray. The cytoplasmic end of the ion conduction pathway is occluded by the presence of the plug helices, but also by the tightly packed side-chains of residue N424. The only Mg^{2+} ion (M1) located in the pore is shown in magenta. (B) Top-to-bottom view of the M1 binding site. Same color representation as in A, the pore-lining side-chains of conserved residue D432 are depicted as stick models.

2.3. Overall structure of MgtE

The membrane-crossing architecture of MgtE is completely distinct among membrane proteins of known structure. This C-terminal TM domain contains five membrane-spanning α-helices per subunit, for a total of ten TM helices in the dimeric assembly (Fig. 1A). TM2, TM3, TM4, and TM5 are arranged as a helical bundle, whereas TM1 engages in domain-swapped interactions with TM2′ and TM3′ from the neighboring subunit (Fig. 1A). The dimeric assembly is stabilized through an extensive interface of hydrophobic and polar interactions within the TM region that are required for MgtE function [39]. Three TM helices from each subunit (TM1, TM2, and TM5) are interlaced around the central ion pore, whereas TM3 and TM4 are more peripheral (Figs. 1 and 2). Numerous glycine and proline residues impart a kinked and slightly twisted appearance on the TM helices and likely contribute to the gating and ion conduction mechanism of MgtE. At a glance, although there is no discernable sequence or functional conservation, the overall architecture of MgtE seems reminiscent of the ATP-binding cassette (ABC) transporter superfamily [68].

A remarkably intimate arrangement of the intracellular domains is found in MgtE (Fig. 1A). This cytosolic region is composed of two structural subdomains: the N-terminal domain (or N-domain) displays a superhelical fold and is followed by a tandem of cystathionine-β-synthase domains (CBS-1 and -2). In a CBS1-to-CBS1 and CBS2-to-CBS2 configuration, the CBS domains of MgtE form a head-to-head interface with the neighboring CBS pair (Fig. 1A). These CBS domains are suspended underneath the TM ion pore through an extended α-helix, nicknamed the plug helix (Fig. 1A). The overall arrangement of the intracellular domains gives the impression that the N-domains are clamped over the CBS domains, which in turn hold the plug helices in place.

The plug helix is a pivotal structural element in MgtE and clearly represents one of the most dramatic examples of a hydrophobic gate observed in an ion channel [69]. Extending from CBS2, these helices occlude the ion conduction pathway at the cytoplasmic end and unambiguously define a non-conductive state. The intracellular regulatory domains may couple structural changes directly through the plug helices to the central ion pore because their covalent link to the TM domain is otherwise observed as an extended structure (Fig. 1A). This unusual gating apparatus serves to highlight the unique topology of MgtE, but it could have broader implications for our understanding of other CBS domain containing channels and transporters, including the ubiquitous ABC and ClC superfamilies [68,64,70].

A striking feature in MgtE is Asp432, contributed by the pore-lining TM5 helix. Asp432 is the only conserved acidic pore-lining residue

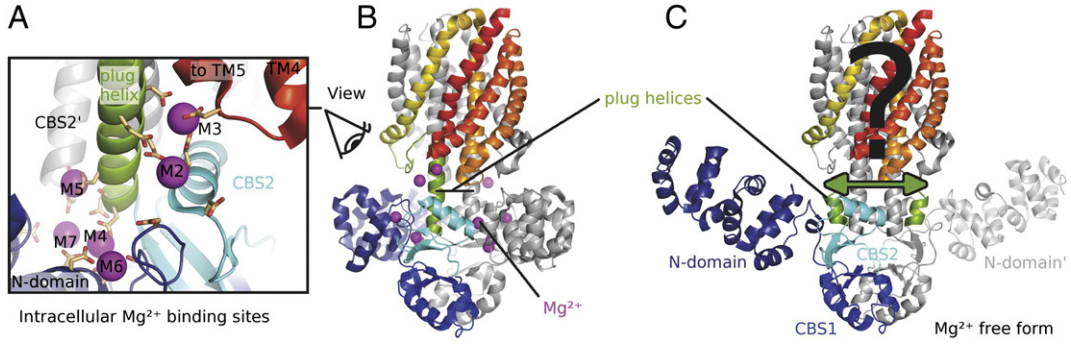

Fig. 3. Gating model for MgtE. (A) Intracellular Mg^{2+} binding sites M2–M7. The direction of the view is indicated by a stylized eye. Only the six sites belonging to one monomer are shown; six more ions bind to the second protomer in an equivalent fashion. The first protomer is shown in rainbow representation, starting with the N-domain in blue and ending with the TM5 domain in red, the second protomer is shown in gray. Mg^{2+} ions are represented by magenta colored spheres. Glutamate and aspartate side-chains involved in Mg^{2+} binding are shown in stick representation. (B) Closed form of full-length MgtE (PDB ID: 2ZY9). Same color coding as in A. (C) Mg^{2+} free form of intracellular part of MgtE (N-domain, CBS domains, partial plug helix, PDB ID: 2YVZ) grafted onto the full-length MgtE structure (PDB ID: 2ZY9). Same color coding as in A/B, with the exception of the partial plug helices of the intracellular part of MgtE (PDB ID: 2YVZ; both in green) and the plug helices of full-length MgtE (PDB ID: 2ZY9; both in gray). The CBS domains of the two structures can be superimposed, but N-domains and plug helices have different relative orientations. These motions suggest a regulatory mechanism in response to loss of intracellular Mg^{2+} ions, probably changing the TM domain architecture towards an open pore by a reorientation of the plug helices (indicated by a green arrow).

found in MgtE and SLC41-type proteins. Nearby electron density in the crystal structure was assigned as a Mg^{2+} ion (M1) held between the Asp432 side-chains from both subunits (Figs. 1 and 2) [38,39]. Subsequent electrophysiological characterization found Asp432 to be essential for MgtE-mediated Mg^{2+} conductance [39], directly implicating this residue in the selectivity and conduction mechanism operating across the entire MgtE family (discussed below).

2.4. Regulatory metal-binding sites

The intracellular domains of MgtE are tied together by bound Mg^{2+} ions. Crystallized in the presence of 200 mM $MgCl_2$, structural analysis revealed twelve Mg^{2+} ions coordinated by highly conserved intracellular acidic residues which link together individual domains of MgtE subunits (Fig. 1C) [38,39]. With six Mg^{2+} ions per subunit (named M2–M7), M2 and M3 are bound near the membrane-proximal interface of the plug helix, CBS2, and TM5 (Fig. 3A–B). M4–M7 ions further connect the intracellular ends of the plug helices, the N-domains, and CBS domains from neighboring subunits. The M2, M4, M5, and M6 ions are involved in direct protein interactions coordinated mainly by glutamate and aspartate side-chains. Coordination distances of slightly less than 4 Å suggest M3 and M7 are bound through water molecules. The dramatic enrichment of acidic residues observed in the intracellular domains would cause a significant repulsion in the absence of bound Mg^{2+} ions, potentially changing the orientation between the N-domains, CBS domains, plug helices, and the TM ion pore. While the high concentration of Mg^{2+} used in the crystallization solution may lead to the identification of some trivial binding sites, these structural findings implicate the intracellular assembly as a potential Mg^{2+}-sensor with a central regulatory role in MgtE channel gating.

2.5. A cytoplasmic structure implicates domain movements

Consistent with impressions gained from the Mg^{2+}-bound full-length MgtE crystal structure, a crystal structure of the isolated intracellular domain from *T. thermophilus* determined in the absence of Mg^{2+} revealed striking domain rearrangements (Fig. 3C) [38]. The N-domain in this apo-structure has disengaged from its interactions with the CBS domains and the plug helix. The CBS2 intersubunit interactions have also disassociated due to electrostatic repulsion generated by the departure of Mg^{2+} ions, and the plug helices have undergone a significant displacement that would effectively "de-cork" these helices from their block of the ion conduction pathway in the full-length channel (Fig. 3B–C). Paramagnetic relaxation enhancement (PRE) experiments have suggested a dynamic interaction between the N-domain and CBS domain in the absence of Mg^{2+} in solution [71] and one anticipates that additional rearrangements within the TM domain would ultimately lead to Mg^{2+} conduction through the MgtE ion pore.

2.6. Insights from molecular dynamics studies

Molecular dynamics (MD) simulations play an increasingly important role in deepening our understanding of membrane protein structure and function [72,73]. MD simulations performed in the presence of Mg^{2+} are consistent with the N-domain of MgtE stabilizing a closed conformation of the CBS domains, with Mg^{2+} ions structurally locking the intracellular domains in a compact conformation [46]. Critically, simulations starting from Mg^{2+}-free models also recapitulate the major features of domain closure upon adding back Mg^{2+} ions into the system. Computational approaches were also used to interrogate the contribution of select Mg^{2+}-binding sites to the overall stability of the intracellular domain assembly. The M5 Mg^{2+} ion, which bridges one plug helix and the CBS2′ domain from a neighboring subunit (Fig. 3A), was reported to be indispensable for maintaining a closed state [46]. Intriguingly, a Na^{+} ion placed at the M5 site was insufficient to maintain the structural lock, indicating that divalent cation specificity exists within the intracellular regulatory domains of MgtE [46]. Moreover, these MD results are consistent with the biochemical observation that only divalent cations, and not Na^{+}, can stabilize MgtE in the presence of exogenously added proteases [46].

2.7. MgtE is a ligand-gated Mg^{2+}-selective channel

In a breakthrough study, electrophysiological characterization of MgtE was accomplished by patch-clamp analysis of spheroplasts generated from MgtE-overexpressing *Escherichia coli* cells [39]. MgtE displayed large conductance and high transport efficiency in Mg^{2+}-containing solutions, consistent with a channel-like conduction mechanism (~100 pS at −40 mV; ~3×10^7 ions/s at −60 mV). Co^{2+} could also permeate through MgtE, but with significantly reduced conductance. This study also definitively demonstrated that intracellular Mg^{2+} within the low millimolar range regulates MgtE activity. Biochemical experiments performed using the purified MgtE protein further supported this conclusion [46]. Concentrations of Ca^{2+}, Na^{+} or K^{+} required to have any measurable effects on MgtE currents were above the physiologically relevant range for these cations, firmly establishing MgtE as a high-conductance Mg^{2+}-selective, Mg^{2+}-gated ion channel [39].

A series of mutant channels were generated to probe the contribution of the intracellular domains to MgtE gating. Mutational crippling of the M5 site (Fig. 3A) abolished Mg^{2+}-dependent regulation, supporting the conclusion that the intracellular domains are responsible for Mg^{2+}-sensing and involved in channel gating. A protein lacking the N-domains showed reduced Mg^{2+}-dependent inhibition as well as an increased open probability, implicating the N-domains directly in MgtE function and regulation. A consistent picture has therefore emerged from genetic, biochemical, structural, computational and electrophysiological analyses that implicate MgtE as a central player in cellular Mg^{2+} homeostasis.

2.8. Insights into ion selectivity and comparison to other channels

Perhaps the most provocative feature of MgtE is its Mg^{2+}-selective ion conduction pore (Fig. 2A–B). It measures ~30 Å in length perpendicular to the plane of the membrane along the central MgtE dimer axis [38,39], where a loop containing acidic residues is expected to concentrate cations near the periplasmic entryway by acting as an electrostatic sink [74]. Since cobalt(III)hexammine, a structural analog of a first-shell hydrated Mg^{2+} ion, is an effective inhibitor of MgtE [39], one might anticipate an initial interaction of hydrated Mg^{2+} ions with MgtE. Hydrophobic residues found just beneath the acidic loop produce a narrow constriction thought to form a periplasmic gate, while the plug helices completely occlude the intracellular end of the ion pore. Crystallographic substitution experiments with Co^{2+} and Ni^{2+} failed to displace the centrally bound M1 site Mg^{2+} ion (Fig. 2A–B), supporting the notion that the ion pore may be blocked from both sides of the membrane in the currently available X-ray structures [39]. Based on limited crystallographic data, a first-shell hydrated Mg^{2+} ion was suggested to be coordinated at the M1 site by the Asp432 side-chains and the carbonyls of Ala428 from both subunits [38]. Alternatively, a partially dehydrated Mg^{2+} ion might be directly bound to Asp432 and the carbonyl of Ala428 from one subunit, as well as through intervening water molecules to the neighboring subunit [38]. The exact details of Mg^{2+} coordination must obviously await higher resolution data and structure determination of MgtE in a conductive state.

Electrophysiological characterization, sequence conservation, and the ion pore structure have implicated the acidic side-chains of Asp432 in the selectivity and conduction mechanism within the MgtE superfamily [39]. Direct or tight binding of permeant Mg^{2+} ions to Asp432 might appear counterintuitive to achieving the high flux rates measured through MgtE. It therefore seems pertinent to consider the potential roles of acidic side-chains that have been increasingly discovered in new ion channel structures despite differences in charge

density, preferred coordination chemistry or water binding properties of the conducted ions.

In a non-conductive, desensitized conformation of the trimeric acid-sensing ion channel (ASIC), three aspartate side-chains participate directly in monovalent ion dehydration and were suggested to play a key role in ion selectivity [75]. However, more recent crystal structures of this channel captured in non-selective (high pH) and Na^+-selective (low pH) conductive forms have found these same aspartate side-chains to surround a much more dilated pore without apparent involvement in ion dehydration [76]. These latest findings suggest that, while ion selectivity is likely influenced by the surrounding electrostatic potential, it may be largely determined by the precise dimensions of a hydrophobic pore (~10 Å radius for the non-selective form and 5 by 7 Å for the Na^+-selective form in ASICs).

Acidic side-chains have been implicated in Na^+ and Ca^{2+}-selective members of the voltage-gated ion channel (VGIC) family, where selectivity filter cross-sections have been estimated to be ~4 by 5 Å in the conductive conformation [77–80]. In the Na^+-selective tetrameric NavAb channel, four glutamate side-chains line the perimeter of a ~4.5 by 4.5 Å ion conduction pathway and were proposed to allow the smaller Na^+ ion to approach these high field-strength anionic sites more closely, permitting faster permeation than other ions [81,82]. However, a repositioning of the selectivity filter glutamate side-chains observed in the tetrameric NavRh Na^+-selective channel relative to NavAb [83], and the ability to convert related bacterial VGICs into highly Ca^{2+}-selective forms by increasing the electronegative character surrounding the selectivity filter [84], collectively serve to reemphasize that electrostatic potential and pore dimensions can decisively combine to give rise to either a Na^+-selective or Ca^{2+}-selective pore.

Themes involving electrostatic potential and pore dimensions are further echoed in the highly Ca^{2+}-selective hexameric calcium-release activated calcium (CRAC) channel. In the CRAC channel, six glutamate side-chains directly line the ion pore entryway to form an intensely electronegative selectivity filter structure with a snug Ca^{2+} coordination site [85]. Mutation of these glutamate residues to smaller aspartate side-chains would undoubtedly widen the selectivity filter, and these mutations are known to concomitantly increase CRAC channel permeability to Na^+ and other monovalent cations [85].

Remarkably, in all known ion channel structures where key acidic side-chains appear to be involved in selectivity (including MgtE), it seems likely that the conducted substrates are probably mostly (or even fully) hydrated cation species. By contrast, highly K^+-selective channels are well known to conduct dehydrated K^+ ions through direct backbone interactions in a long, narrow, carbonyl-lined filter [86,87]. Ironically, the historic K^+ channel structural example of a selectivity filter whose architecture and chemistry have been optimized through evolution to mimic the first hydration shell of its substrate (the K^+ ion) is proving to be more likely the exception rather than the rule in selective cation channels. Any paradox here is resolved upon considering the relative free-energies of hydration since K^+ ions are at one end of the spectrum and the smaller, more charge-dense Na^+, Ca^{2+} and Mg^{2+} ions lie towards the other. For the latter, excessively removing waters of hydration might be too energetically expensive to achieve high conductance rates, and this seems especially true for the Mg^{2+} ion. Although more studies are required to determine the underlying detailed components of selectivity and conduction in MgtE, we speculate that a combination of precise pore dimensions and electrostatics will achieve Mg^{2+} selection at the universally conserved and essential Asp432 side-chains, perhaps through direct, partial dehydration.

3. CorA

3.1. Distribution of the CorA system

CorA was named for the cobalt-resistant mutants in which it was first identified [34,35]. Maguire and colleagues subsequently cloned the *corA* genes from *Salmonella typhimurium* and *E. coli* [88–90]. A complex relationship between *corA* transcription, protein abundance and Mg^{2+} influx has been established [91]. Modulation of CorA expression by RNase III activity has also recently been demonstrated [92]. The available data suggest that CorA is regulated in vivo, but the underlying mechanisms are not yet completely understood. Underscoring its importance in microbial physiology, *corA* is an essential gene in *Haemophilus influenzae* [93], required for full virulence of *Salmonella* [91,94,95], and found in approximately half of all sequenced prokaryotic genomes [96]. *corA* and *mgtE* are often present with other microbial Mg^{2+} transport systems (Table 1), although both are rarely encoded within the same genome. Like MgtE, CorA is presumed to function as the primary cellular Mg^{2+} transport system.

A somewhat ambiguous nomenclature for the CorA family has emerged where at least two *corA* subgroups and a third *corA*-like gene (called *zntB*) have been described [36,97–99]. The so-called "class A" CorA protein from *Thermotoga maritima* (TmCorA) can mediate Mg^{2+} uptake [47] but has been suggested to function as a Co^{2+}-specific influx system *in vivo* [45,100]. ZntB, by contrast, has been characterized as a putative Zn^{2+} effluxer that presumably does not play any role in Mg^{2+} import [98,99]. Extensive phylogenetic analysis of the CorA superfamily also implies a functional divergence at many levels [36]. For example, four *corA*-like genes can be identified within the genome of the bacterium *Cupriavidus metallidurans*, which lives in metal-rich environments, suggesting different and specialized roles in metal flux for members of this protein superfamily [36]. CorA proteins likely contribute to metal hypersensitivity [101–104] and have been described to mediate the efflux of Mg^{2+} under certain conditions [90], although this latter point remains controversial. Rigorous functional characterization is therefore required to define each CorA-like protein and this represents an important area of future research.

In eukaryotes, the CorA-like Mrs2 protein is found in mitochondrial inner membranes [105–108]. Mrs2 is required for normal mitochondrial Mg^{2+} homeostasis and function, the stability of mitochondrial respiratory complexes [109–111], and the maintenance of myelination within the central nervous system [112,113]. Notably, *mrs2* expression is a genetic hallmark of embryonic stem cells [114] and its overexpression has been linked to a multidrug resistance phenotype in cancer [115,116]. The yeast CorA-like plasma membrane proteins Alr1 and Alr2 have been implicated in cellular Mg^{2+} homeostasis and translation fidelity [117–121], whereas the vacuole-residing Mnr2 protein regulates intracellular Mg^{2+} stores [122]. In plants, the CorA family has undergone a significant expansion and these CorA-like proteins likely participate in divalent cation transport across many different cellular membranes [36]. In *Leishmania major*, an intracellular parasite, it is remarkable that two *corA*-like gene products appear to play opposing roles in virulence [123]. The CorA–Mrs2–Alr1 superfamily therefore has significant and highly specialized roles in the biology of divalent cation transport.

Using electrophysiological methods, the Alr1 and Mrs2 proteins have been characterized as high-conductance Mg^{2+}-selective channels [120,124]. It is notable that distant members of the CorA–Mrs2–Alr1 superfamily can complement for one another in heterologous expression systems, supporting the notion of a conserved structural architecture and ubiquitous functional conservation [105,107,119,123,125,126]. In fact, the CorA–Mrs2–Alr1 superfamily is recognized by a signature glycine–methionine–asparagine (GMN) motif that is known to be essential for channel function and stability [36,47,124]. Hetero-oligomeric complexes with distinct transport capacities have also been described [108,121], which suggests that an even broader functional divergence may exist across the CorA–Mrs2–Alr1 superfamily.

3.2. Structure determination of CorA and related proteins

Three independent research groups almost simultaneously reported crystal structures of *T. maritima* CorA (TmCorA) in the presence of Mg^{2+} or Ca^{2+} at 2.9, 3.7 and 3.9 Å resolution, respectively [40–42]. The choice

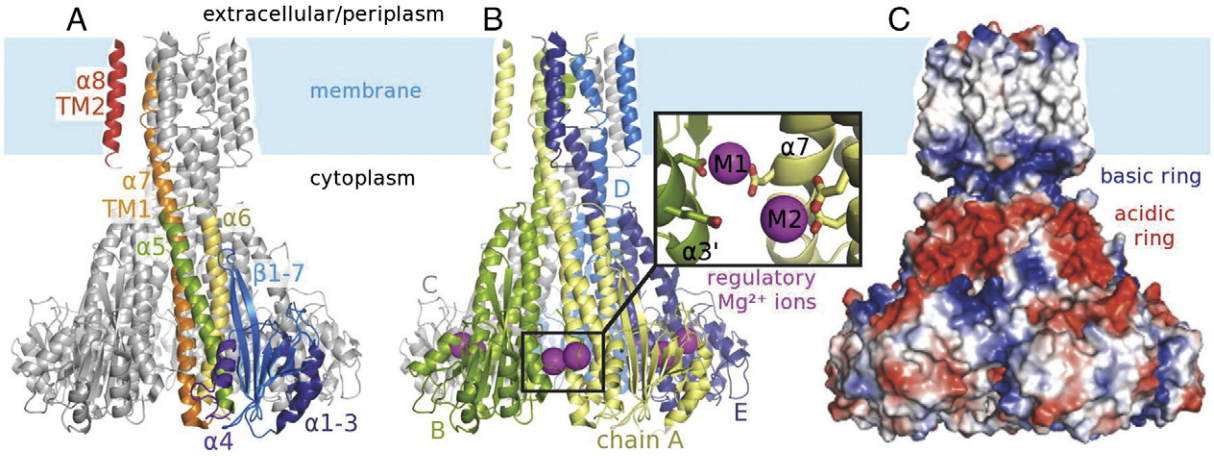

Fig. 4. Overall structure of the CorA Mg^{2+} channel in a closed state. The illustrations are representative for all crystal structures of full-length or nearly full-length *Thermotoga maritima* CorA obtained with divalent cations (PDB IDs: 2BBJ, 2IUB, 2HN2, 4EED), the differences to *Methanocaldococcus janaschii* CorA and the effects of monovalent ions are discussed below. (A) In one protomer of the TmCorA pentamer, different colors indicate various structural regions: α-helices α1–α3 (deep blue), β-sheets β1–β7 (marine), α4 (purple), α5 (green), α6 (yellow), the extremely long α-helix α7 (orange), and finally α8 (red) with the C-terminus located back in the cytoplasm. (B) The five protomers (chains A–E) are shown in different colors. Ten divalent cations are located around the periphery of the funnel domain, two (M1 and M2) between each protomer–protomer interface. Additional ions in the pore are discussed below. (C) Electrostatic surface features displayed with red representing acidic regions and blue representing basic regions. A concentration of acidic side chains forming an "acidic ring" contributed by α5/α6 residues abuts a "basic ring" contributed by TM1/TM2 residues. Although partially obscured in this view, the M1/M2 metal binding surfaces are also intensely negatively charged.

of detergent proved to be essential for obtaining the highest diffraction quality crystals [41], a feature common in membrane protein crystallography. TmCorA was revealed to be a funnel-shaped homopentamer with a large intracellular N-terminal domain linked through an extended α-helix to a C-terminal transmembrane (TM) ion pore domain (Fig. 4A). Although TmCorA also contains a total of ten TM α-helices (two contributed from each subunit) and a large intracellular domain, its primary sequence and overall structure are completely unrelated to MgtE.

When crystallized in the presence of 100–300 mM $MgCl_2$, $CaCl_2$, or $Mg(NO_3)_2$, divalent cations were identified along the central ion pore and bound between neighboring subunits of TmCorA (Fig. 4B). The intracellular domains were therefore assumed to fulfill an important regulatory role because direct metal coordination through conserved acidic side-chains was observed at the subunit interface. Overall, the three initial TmCorA structures were highly similar, 5-fold symmetric, and thought to represent a closed conformation of the ion channel. Recently, the full-length crystal structure of CorA determined in the presence of 60 mM $MgCl_2$ from the archaeon *Methanocaldococcus jannaschii* (MjCorA) has also been reported [43].

Following a common strategy used in membrane protein structural biology [127], crystal structures of the isolated intracellular domain from a number of CorA homologs have also been determined [40,42], including two structures of intracellular domains from ZntB [128,129]. These studies have resulted in different conformational changes being proposed as the gating mechanism for this unique class of divalent

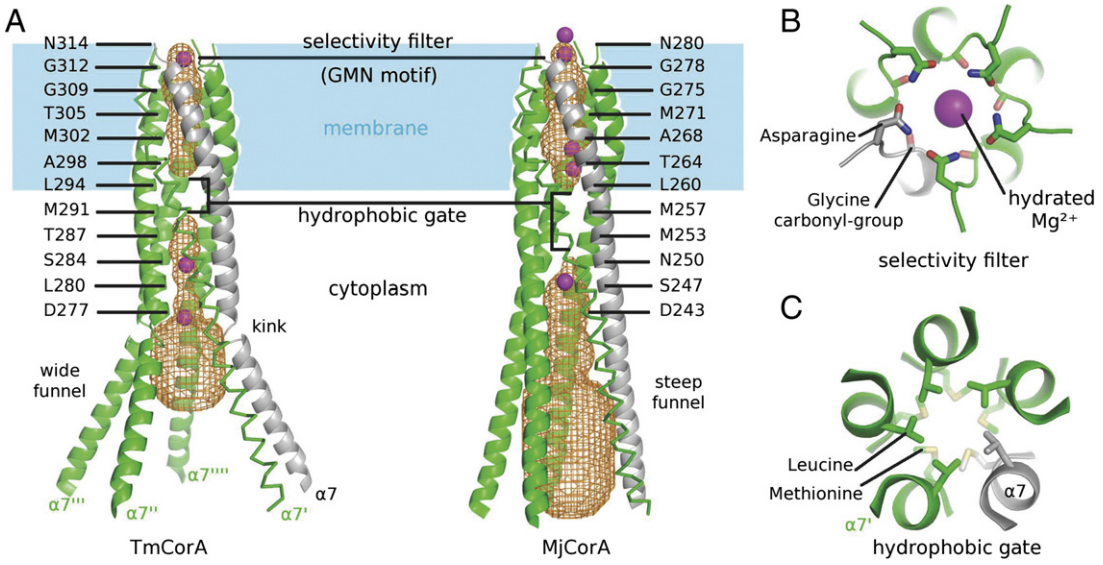

Fig. 5. Structure of the CorA ion pore. (A) For both TmCorA (PDB ID: 4EED) and MjCorA (PDB ID: 4EV6), only the pore forming helix α7 is shown, with chain A in gray and chains B–E in green. Pore lining residues are indicated for both homologues. Mg^{2+} ions are represented by magenta colored spheres. The solvent accessible pore volume calculated by MOLE [165] is rendered as an orange mesh. Note that in both cases a portion of the ion conduction pathway is inaccessible to water molecules (hydrophobic gate), indicating a non-conductive state. (B) Top-to-bottom view of the selectivity filter (GMN motif) in TmCorA. Side-chains of N314 and carbonyl groups of G312 are shown in stick representation. The selectivity filter in MjCorA is virtually identical. (C) Top-to-bottom view of the hydrophobic gate in TmCorA. Side-chains of residues L294 and M291 are depicted as stick representation. The hydrophobic gate in MjCorA is similar but even more occluded by five additional methionine side-chains from M253.

cation transport proteins [42,47,49,129]. Critically, the N-terminal domain of yeast Mrs2 (PDB ID: 3RKG; [130]) superimposes well with the corresponding regions of CorA and ZntB. Therefore, opposing earlier claims [97,131], this finding supports the concept that the entire CorA–Mrs2–Alr1 superfamily shares the same general structural scaffold despite limited sequence identity.

Wild-type TmCorA has so far resisted all crystallization efforts in the absence of divalent cations. Following protein-engineering efforts, crystal structures of a nearly full-length TmCorA channel (TmCorA-ΔNcc;ΔN25/R222A/K223A mutant) could be determined in both the presence and absence of Mg^{2+}. These new TmCorA-ΔNcc structures have revealed key regulatory domain motions that are communicated to the ion pore, in addition to the binding mode of a hydrated Mg^{2+} ion to the GMN motif at the extracellular entryway of the pore [44].

3.3. Overall structure of CorA

The architecture of CorA is unique among membrane proteins of known structure, although TmCorA and MjCorA both form homo-pentamers with a similar overall structure. Within their transmembrane regions, five TM1 helices generate an ~55 Å long centrally located ion pore with the conserved GMN motif that defines the CorA–Mrs2–Alr1 superfamily lining the extracellular pore entrance (Figs. 4 and 5) [36]. Five short extracellular loops between TM1 and TM2, best resolved in MjCorA, form a polar bowl surrounding the mouth of the ion pore. TM2 ends back in the cytoplasm with a conserved intracellular sequence enriched in basic residues (KKKKWL in TmCorA and RRSGWL in MjCorA). Together with basic side-chains contributed by TM1, this remarkable basic ring (BR) feature forms a cuff around the intracellular end of the ion pore where it creates an intense electropositive potential (Fig. 4C). Unlike the intimately interwoven pore-forming TM1 helices, the peripheral TM2 helices of CorA are more loosely associated with the central ion pore and may have more dynamic interactions within the membrane lipid bilayer (Fig. 4) [40–42,48,49,132]. Although unrelated at the primary sequence level, the TM architecture of CorA is reminiscent of the pentameric ligand-gated ion channel superfamily [133,134] and the recently characterized SLAC1 family of anion channels [135].

The TM domain of CorA is elaborated by striking extensions of the TM1 helices (α7 in TmCorA) that support the entire intracellular funnel domain assembly (Fig. 4A). For consistency, this review will use the TmCorA helix numbering throughout, although the TmCorA α1-helix equivalent in MjCorA adopts a loop structure. The intracellular domain of CorA is composed of a central β-sheet flanked by two or three small α-helices on one side (α1, α2 and α3 in TmCorA) and three longer α-helices on the other (α4, α5 and α6 in TmCorA; Fig. 4A). In both TmCorA and MjCorA, the outer surface of the intracellular funnel domain is decorated with acidic residues contributed by α5 and α6 that form a strong acidic ring (AR) feature, which juxtaposes the aforementioned basic ring (BR) element (Fig. 4C). These conserved electrostatic features of CorA have been suggested to play a variety of roles in gating [40,42,44,47,49,132].

3.4. Regulatory metal-binding sites and related domain motions in TmCorA

An intrinsic, intracellular Mg^{2+} sensor has been identified within the funnel domain of TmCorA. Five primary regulatory M1 ions assigned as Mg^{2+} or Ca^{2+} (the cations present during crystallization) are coordinated directly between the side-chains of Asp89 (α3) and Asp253 (α7′) from a neighboring subunit [40–42] (Fig. 4B). At the subunit interface, five additional divalent cations are bound through water molecules at the M2 site (Fig. 4B) [41,42]. The strategic positioning of these ten bound divalent cations symmetrically around the CorA pentamer suggested that they represent key regulatory sites. In addition to Mg^{2+} and Ca^{2+} [40,42], Co^{2+} has also been observed to bind CorA in this region [41], suggesting the possibility of competition between intracellular cations. Although the physiological concentration of each ion must be considered, the details of ion coordination differ among divalent cations [40–42] and may have distinct functional consequences for CorA. Notably, a contribution of the five M1 sites to TmCorA regulation has since been demonstrated using cellular complementation and liposomal Mg^{2+} flux assays [47].

Since they shield an otherwise electrostatically repulsive interface (Fig. 4B–C), disassociation of the bound M1 and M2 metals under conditions of Mg^{2+} deprivation could propagate significant structural changes throughout TmCorA. Supporting this idea, the purified TmCorA protein is protected from proteolysis in a divalent cation-dependent manner, and this protection occurs at concentrations which suggest that Mg^{2+} is the only physiologically relevant intracellular regulatory ion (i.e. at 0.05–2 mM) [42,47]. Furthermore, monovalent cations completely fail to protect TmCorA from proteolysis in this assay [42,47]. More recently, the structure of TmCorA-ΔNcc in the absence of divalent cations has shown monovalent ions bound less tightly, with irregular occupancy, and through water molecules at the M1 and M2 sites (see Fig. 7) [44]. TmCorA-ΔNcc further revealed a series of nonequivalent rigid-body motions among individual subunits leading to the development of a markedly structurally asymmetric CorA pentamer. These findings confirm that monovalent cations are not able to lock CorA in a five-fold symmetric, closed state (Fig. 7). It was proposed that protein-engineering stabilized TmCorA-ΔNcc in an intermediate conformation between open and closed states; yet molecular dynamics simulations also support the notion that loss of intracellular Mg^{2+} ions at the subunit interface will trigger an asymmetric conformational wave throughout the pentameric assembly [44].

Five bound chloride ions have also been assigned within the intracellular domain of TmCorA [41]. Any role for these anions remains unclear. Notably, the pentameric intracellular funnel domain structure from *Vibrio parahemolyticus* ZntB (VpZntB) displayed twenty-five bound chloride ions, and the electrostatic influence of these anions was suggested to develop divalent cation selectivity in this putative Zn^{2+} effluxer [128]. If such a mechanism to achieve ion selectivity proved to be operational in VpZntB, this finding would have profound implications beyond the CorA superfamily. Curiously, the pentameric intracellular domain structure from *S. typhimurium* ZntB (StZntB) revealed numerous bound Zn^{2+} ions, with absolutely no bound Cl^{-} ions [129]. Therefore, whether monovalent cations or anions play any physiological role in regulating CorA function remains to be determined.

3.5. Regulatory metal-binding sites and intermediate state of MjCorA

The structure of MjCorA crystallized in the presence of Mg^{2+} differs markedly from wild-type TmCorA crystallized under similar conditions. The extended, intracellular portion of "α7" (actually α6 in MjCorA, see above) has straightened significantly in MjCorA. This is, in part, clearly due to a stabilizing effect of end-to-end packing of related channel molecules within the MjCorA crystal lattice [43]. This straightening of α7 brings about an overall reorientation and slight repacking of the intracellular regulatory domain in MjCorA relative to TmCorA. Consequently, the M1 divalent cation binding site is not formed in MjCorA since the equivalent α3 coordinating aspartate residue (Asp54) has been displaced ~15 Å from its would-be mate on α7′ (Asp219) (Fig. 6).

In stark contrast to the symmetric, Mg^{2+}-bound structure of TmCorA [40–42], individual subunits of the Mg^{2+}-bound MjCorA are found in a surprisingly asymmetric arrangement [43]. Given our recent structural and functional analysis of TmCorA-ΔNcc, we propose that packing of MjCorA within its crystal lattice has frozen-out an intermediate state of MjCorA somewhere along the trajectory between the closed and open conformations, in spite of the crystallization condition containing 60 mM $MgCl_2$. In this light, we believe that it is especially informative to compare the structures of MjCorA and TmCorA.

Unlike in the Mg^{2+}-bound TmCorA structures [40–42], intracellular Mg^{2+} ions are asymmetrically bound and interdigitated throughout the

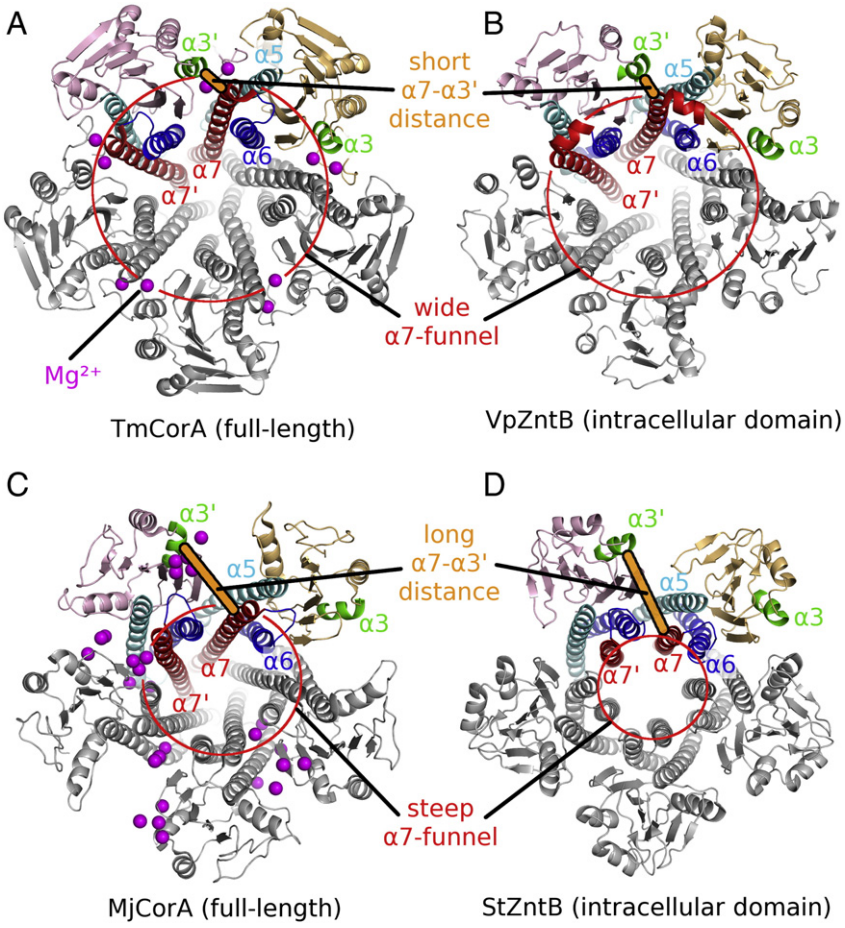

Fig. 6. Pentameric structures of various CorA and ZntB homologues. Bottom-to-top view from the intracellular channel side along the pore axis. The same helix nomenclature (α3, α5, α6, α7) and color coding is used for all structures to indicate corresponding helices. Two neighboring protomers are colored, the remaining three protomers are shown in gray. An orange bar indicates the distance between helices α7 and α3′. A red circle connects the N-termini of the five α7 helices and marks the bottom of the intracellular funnel. The size of the circle indicates the steepness of the intracellular funnel, a side-view of the CorA funnel is provided in Fig. 5A. Mg^{2+} ions are represented by magenta colored spheres. A large diameter α7 funnel seems to correlate with a short α7–α3′ distance, and vice versa. Since in TmCorA the short distance between α7 and α3′ is bridged by Mg^{2+} ions, these conformational differences might be related to regulation and gating. (A) TmCorA (PDB ID: 2IUB, chains F–J). (B) VpZntB (PDB ID: 3CK6). (C) MjCorA (PDB ID: 4EV6). (D) StZntB (PDB ID: 3NWI).

regulatory domains of MjCorA. More remarkably, all of these Mg^{2+} ions appear to bind MjCorA through their first hydration shells, implying that the intracellular domains of CorA have an intrinsic ability to sense and concentrate hydrated Mg^{2+} ions. Therefore, once freed from the constraints of its crystal lattice (see above), perhaps direct engagement and partial dehydration of these Mg^{2+} ions could lock MjCorA into a symmetric, Mg^{2+}-bound closed state through side-chain interactions analogous to those found at the M1 site in TmCorA (Fig. 6). Regardless of the mechanistic details, the CorA–Mrs2–Alr1 proteins have emerged as a superfamily of ligand-gated ion channels where the intracellular ligand (Mg^{2+}) acts as a negative regulator. Unlike MgtE, the oligomeric arrangement of the intracellular regulatory domains in CorA and their direct structural-coupling to the pore-lining TM1 helix is reminiscent of the intracellular gating apparatus found in the Ca^{2+}-activated K^+ channels [136,137].

3.6. Insights from cytoplasmic structures

An early intracellular soluble domain structure from *Archeaoglobus fulgidus* CorA (AfCorA) had recapitulated the architecture of TmCorA, but when grafted onto TmCorA, α6 was seen to rotate around α7 and α5 flipped around the α5–α6 loop [42]. These rearrangements hinted that disassociation of divalent cations from their intracellular binding sites might produce gating events along the ion pore by imparting torque along TM1. Although much less dramatic than first suggested by AfCorA, this type of gating scenario is realized when the full-length crystal structures of TmCorA, TmCorA-ΔNcc and MjCorA are compared (Figs. 6–7).

It should be pointed out that structures of isolated domains from integral membrane proteins have been known to produce suspect or non-physiologically-relevant assemblies [138,139]. In fact, this is the case for a number of CorA and ZntB constructs [40,42,43,131,140], so drawing firm conclusions about the gating mechanism must be weighed against multiple lines of evidence. Nevertheless, the intracellular domain structures of ZntB may offer relevant insight into CorA gating events [128,129]. For instance, the helical packing of α5, α6 and α7 seen in the VpZntB pentameric assembly closely approximates the arrangement found in MjCorA, yet VpZntB also maintains a direct α3–α7′ interface (Fig. 6). This observation could support the proposal that MjCorA is competent to coordinate intracellular divalent cations directly through acidic side-chains (perhaps through an α3–α7′ interface) as seen in the symmetric, Mg^{2+}-bound, closed state structures of full-length TmCorA.

3.7. The CorA ion pore and gating

The CorA ion pore is unlike that of any other ion channel characterized to date. However, the recently determined CRAC channel pore

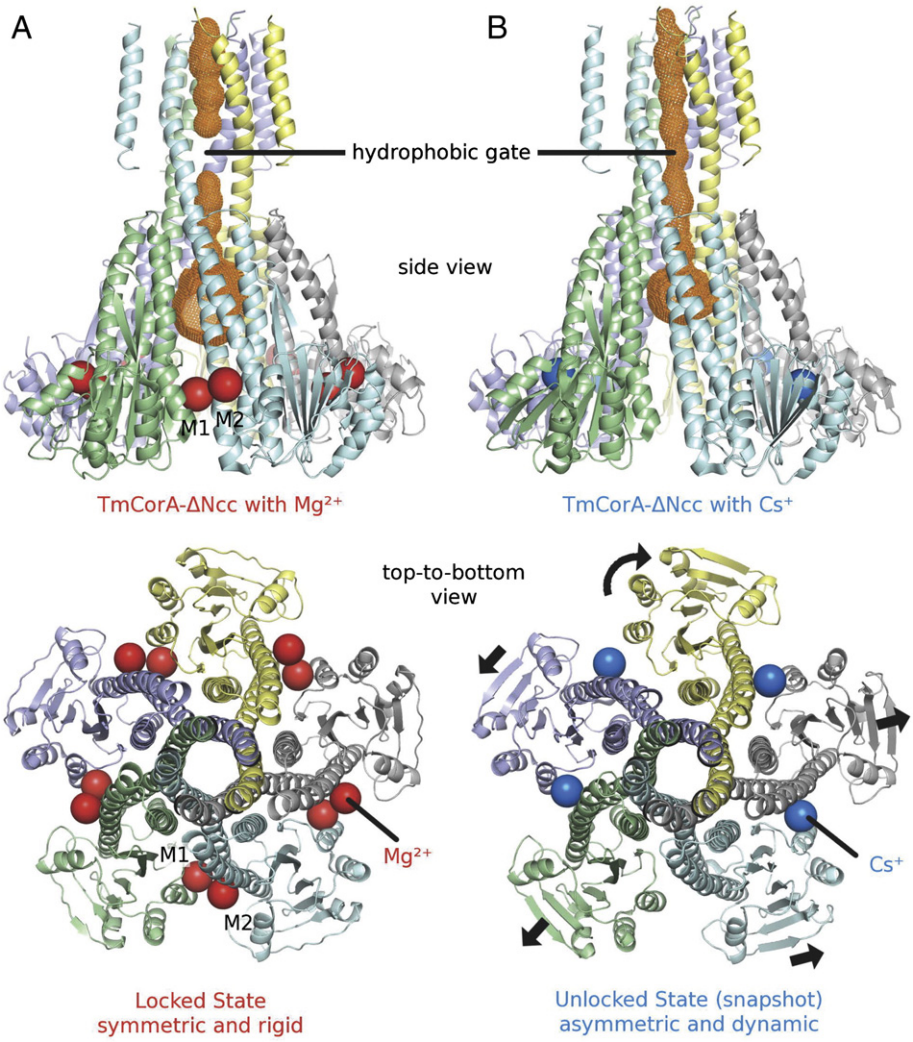

Fig. 7. Gating model for CorA. (A) Crystal structure of TmCorA-ΔNcc in the presence of 200 mM Mg^{2+} (PDB ID: 4EED). (B) Crystal structure of TmCorA-ΔNcc in the presence of 50 mM Cs^{+} (PDB ID: 4EEB). Black arrows indicate the movements of the individual protomers in the Cs^{+}-bound form. Protomers A–E are shown in gray, aquamarine, green, violet, and yellow, respectively. The solvent accessible pore volume (shown in orange) was calculated by MOLE [165]. In the absence of Mg^{2+}, the hydrophobic gate is slightly widened, and the entire pore is now water accessible.

shares a number of unanticipated similarities, including a similar overall length, a central hydrophobic gate, and an intracellular electropositive barrier to cation flow [85]. Two of the most profound features of the CorA ion pore are the absence of conserved acidic residues along the conduction pathway, and its surprising overall length of ~55 Å. Detailed analysis of the pore reveals a hydrophobic stretch that is too narrow to permit the passage of a single water molecule (Fig. 5), enforcing the conclusion that the TmCorA and MjCorA structures have been captured in closed or non-conductive states. Still, portions of both pores are wide enough to accommodate a Mg^{2+} ion with its first hydration shell intact (Fig. 5) [40–44,49]. From all of the available CorA crystal structures, a total of eight divalent cations have been assigned along the ion pore (Fig. 5). In fact, MjCorA appears to house up to five hydrated Mg^{2+} ions simultaneously (Fig. 5) [43]. This implies that CorA contains a functional multi-ion pore, and this result immediately invokes the possibility of a knock-on conduction mechanism [141,142].

One captivating feature about CorA is the universally conserved, essential and unique GMN motif that lines the extracellular pore entryway. In both TmCorA-ΔNcc and MjCorA structures, a bound Mg^{2+} ion is coordinated through its first shell of waters to the asparagine sidechains and glycine backbone carbonyl atoms at the GMN motif (Fig. 5B) [43,44]. This interaction is notably asymmetric with respect to the central pore axis, as are all Mg^{2+} coordination sites observed within the CorA pore (Fig. 5B) [43,44]. These structural observations serve to define the GMN signature sequence as the selectivity filter in the CorA–Mrs2–Alr1 superfamily, but an analogous Mg^{2+} site had not been observed in previous TmCorA structures [40–42]. This still unexplained discrepancy implies that the loss of symmetric Mg^{2+} binding to the intracellular regulatory domains, or the ensuing asymmetry that develops along the ion pore, may be a prerequisite to activate the CorA selectivity filter to become permissive to ion conductance [44].

A remarkable characteristic of the CorA pore is an intense electropositive potential contributed by the so-called basic ring (BR) that surrounds the ion pores' intracellular end (Fig. 4C). This feature was initially proposed to function as an electrostatic gate [40], and such a design will ensure tight regulation under normal physiological conditions to avoid unwanted cation influx. Computational studies indeed support the notion that the BR presents an insurmountable energetic barrier to Mg^{2+} influx starting from the Mg^{2+}-bound pore structures of TmCorA [49,132]. Conformational changes of CorA associated with transitions towards the presumed conductive state suggest that partial neutralization of the BR might occur through interactions with sidechains of the acidic ring (AR) or surrounding membrane lipid headgroups [44].

It was initially surprising to find a long hydrophobic stretch within the CorA pore, especially considering the unique chemistry of Mg^{2+}.

In TmCorA-ΔNcc and MjCorA, one now observes polar side-chains and backbone carbonyls playing crucial roles in coordinating hydrated substrates along the pore. These findings serve to largely offset the energetic (and conceptual) challenges associated with conducting a charge-dense substrate like the Mg^{2+} ion. Nevertheless, hydrophobic gates are found in a wide variety of membrane transport proteins [69] and one is implicated in TmCorA function [40–42,47,49,132,143]. For instance, mutation of the pore-lining Leu294 side-chains into smaller hydrophobic residues leads to an increased transport capacity, which is also communicated to the intracellular regulatory metal binding sites. Although separated by nearly ~60 Å in TmCorA, a reciprocal communication pathway is presumed to exist between the intracellular regulatory sites and the hydrophobic gate in CorA.

It is generally expected that a hydrophobic ion pore must become at least partially wetted in order to conduct ions [144,145]. Not surprisingly, computational analyses have indicated an energetic barrier to ion conductance at the hydrophobic gate in TmCorA [49,132]. Supporting the assignment of TmCorA-ΔNcc and MjCorA structures as gating intermediates, extended molecular dynamics simulations performed in the absence of intracellular regulatory metals lead to stable hydration within this pore region [44,49]. Nevertheless, it is still remarkable that the slight pore dilations associated with the asymmetric arrangements of the TM1 pore-lining helices seen in TmCorA-ΔNcc and MjCorA appear so robustly suited to house hydrated Mg^{2+} substrates [43,44]. This suggests an energetic balance whereby CorA is optimized to selectively load its long ion pore with multiple (at least partially) hydrated Mg^{2+} ions while maintaining a non-conductive state. In the CorA conductive state, perhaps a further slight rotation of the TM1 helix along the hydrophobic stretch will either bring conserved polar side-chains into the ion pore or displace hydrophobic side-chains away from the conductance pathway to initiate high-capacity influx of hydrated Mg^{2+} ions.

3.8. Insights into ion selectivity and conductance

Until recently, the structural basis of ion selectivity in the CorA–Mrs2–Alr1 superfamily had remained a mystery. It is now clear that the conserved GMN motif lining the pore entryway supports the selection of first shell hydrated Mg^{2+} ions through soft side-chain (via Asn) and backbone carbonyl (via Gly) interactions. So far, this selectivity filter structure and mechanism are unique among membrane proteins of known structure, but it is somewhat reminiscent of the partially hydrated Ca^{2+} ion seen coordinated to the backbone carbonyls within the selectivity filter of the NavRh channel [83].

CorA has apparently evolved to select and conduct hydrated versions of its charge-dense Mg^{2+} substrate. This solution intuitively makes sense because excessively removing the first hydration shell from Mg^{2+} would be most demanding energetically and counterproductive to achieving high flux rates. At its selectivity filter, CorA therefore exploits the unique, slowly exchanging water structure of the Mg^{2+} ion by using soft chemical ligands precisely arranged to recognize the decisively strict coordination geometry of Mg^{2+}. When considering the radii of the first hydration shell (2.1 Å for Mg^{2+}), this scenario also predicts why CorA might conduct the similar sized Co^{2+} and Ni^{2+} ions (2.08 Å and 2.06 Å, respectively) but excludes the larger Ca^{2+} ion (2.46 Å) [1–3,146]. This setting can further explain why cobalt(III) hexammine, a structural analog of a first shell hydrated Mg^{2+} ion, is an effective inhibitor of the CorA superfamily [47,124], but why larger analogs are not [147]. This intriguing hypothesis also suggests that slight structural changes at the selectivity filter of CorA might disfavor Mg^{2+} binding and lead to a transient disassembly of the presumed conductive multi-ion pore configuration. We speculate that structural fluctuations at the selectivity filter could therefore represent an effective mechanism to precisely control and regulate Mg^{2+} flux through CorA.

Multiple hydrated Mg^{2+} ions are seen along the MjCorA ion pore, including one extracellular to the GMN motif coordination site (Fig. 5A). This key structural observation suggests that an incoming substrate will promote rapid ion conduction through a knock-on conduction mechanism since hydrated Mg^{2+} ions are corralled and aligned within the long CorA ion pore. Paradoxically (see below), this proposed mechanism of ion selectivity and conduction conceptually is somewhat reminiscent of K^+ channels, where backbone carbonyls are perfectly arranged to mimic the first hydration shell of K^+ ions that permeate in a multi-ion configuration [86,87].

Until recently, it had generally been assumed that direct ion–protein contacts would be required to confer high selectivity in ion channels [142]. In K^+ channel selectivity filters, for example, low field-strength anionic carbonyl sites appear well suited to directly dehydrate incoming K^+ ions with little energetic penalty [86,87]. By contrast, structural analysis of the SLAC1 anion channel has clearly revealed a selectivity sequence correlated with the free energy of ion hydration where substrates that are more easily dehydrated are more permeant, without implicating direct ion–protein interactions [135]. An analogous proposal has been suggested for the ligand-gated pentameric ion channel family following structure determination of the GluCl anion channel [148]. It therefore seems unique and remarkable that the CorA superfamily may achieve high selectivity without direct ion–protein interactions for an ion that holds on to its hydrating waters more tightly than all others (as is the case for the Mg^{2+} ion).

Additional structural components are likely involved in achieving or tuning selectivity in the CorA–Mrs2–Alr1 superfamily. The extracellular loop connecting TM1 to TM2 contains highly conserved acidic side-chains suggested to directly coordinate and concentrate Mg^{2+} ions near the mouth of the pore [132,149]. These acidic residues are associated with high capacity flux [121,124], but they are not essential for CorA function [42,47,49,150]. Others have indicated the existence of weaker binding sites for hydrated Mg^{2+} ions along the extracellular loop [48,49]. Since the first hydration shell of Mg^{2+} is in slow exchange, CorA may begin to achieve selectivity at this extracellular surface. This type of initial interaction would not incur the energetic penalty of partially dehydrating the Mg^{2+} substrate, which is consistent with high conductance rates [120,124]. It has also been reported that the extracellular loop is important for stabilizing CorA [47,151] and it is reasonable to assume that this region helps to maintain the overall architecture of the selectivity filter during gating.

3.9. CorA is a ligand-gated Mg^{2+}-selective ion channel

The probability of the Mrs2 channel to occupy its open conformation is known to respond to the effective Mg^{2+} concentration [124], and divalent cations identified between subunits first suggested that CorA might be regulated by intracellular Mg^{2+} [40–42]. Subsequent biochemical analysis indicated that the Mg^{2+} ion can maintain TmCorA in its closed conformation at physiological concentrations [42,47], implying the intracellular funnel functions to sense the free Mg^{2+} concentration and gate the ion pore to maintain cellular Mg^{2+} balance. Conserved acidic residues on both the interior and exterior sides of the funnel domain appear to effectively concentrate hydrated intracellular Mg^{2+} ions, ensuring that CorA can efficiently survey the available free intracellular Mg^{2+} concentration at all times. Perhaps it is not surprising that an ion channel poised to potentially permit the influx of toxic cations like Co^{2+} and Ni^{2+} into the cell would be tightly regulated. In its closed state, the CorA ion pore contains at least two additional built-in safety measures: a hydrophobic gate and an intracellular electropositive gate. Both of these pore features likely function in concert with the intracellular regulatory domains of the subunits to ensure regulated influx of metals through CorA.

It is important to emphasize that multiple *in vivo* and *in vitro* studies indicate that the CorA, Alr1 and Mrs2 proteins function as ion channels, moving Mg^{2+} into the cell (or mitochondria) based on the driving force supplied by the membrane potential [47,106,108,120,124,152]. Nevertheless, members of the CorA superfamily have also been suggested to function as metal transporters or effluxers [36,41,97,98]. It is not

immediately obvious how such functional diversity might fit onto the CorA framework, and these open questions remain a compelling area for future investigation. If both channel and transporter mechanisms indeed operate on a conserved CorA-like scaffold, this scenario may be reminiscent of the ClC superfamily where channel-like members are thought to function through a defunct transporter mechanism [153,154].

3.10. Molecular dynamics studies of CorA

In addition to identifying the hydrophobic gate, computational studies on TmCorA have defined energy wells associated with metal binding along the ion pore (Fig. 5A) and suggested that acidic residues in the extracellular loop attract and stabilize cations near the pore entrance [49,132,149]. The intracellular basic ring (BR) was also found to exert a large barrier to ion permeation (Fig. 4C), implying that a significant repositioning or shielding of these basic residues is required for ion conduction [49,132]. Consistently, mobility of the TM2 segment has been noted [42,48,49,132] and extended MD simulations performed in the absence of regulatory Mg^{2+} ions result in significant charge neutralization and repositioning of the BR. MD simulations have further demonstrated a reorientation of the intracellular domains to be correlated with dilation and wetting of the pore in the absence of regulatory Mg^{2+} ions, reflecting the findings of the TmCorA-ΔNcc crystal structure analysis [44,49]. Overall, computational studies indicate that correlated movements occur throughout CorA during gating in response to low intracellular Mg^{2+} concentrations and that Mg^{2+} passes through a wetted CorA pore in a hydrated form.

4. Summary

4.1. MgtE and CorA are non-identical twins

Until recently, the structural basis for selective, regulated Mg^{2+} transport in biology has remained a complete mystery. MgtE and CorA have since provided compelling insights and revealed a number of shared attributes built upon entirely distinct structural scaffolds. Residues that act to increase the local Mg^{2+} concentration, potentially by promoting interactions with hydrated ions, surround the pore entryways of both channels. In this way, Mg^{2+}-selective transport systems may begin to exploit the unique water binding properties of Mg^{2+} to improve ion selectivity. Perhaps unexpectedly, MgtE and CorA are also found among a growing class of structurally characterized ion channels that have selectivity filters wide enough to accommodate hydrated substrates (including ASICs, NavAb, SLAC1 and GluCl). We now know that the selectivity filters and pore structures in MgtE and CorA can both easily accommodate Mg^{2+} ions with their first hydration shells intact, suggesting that these ion channels conduct at least partially hydrated Mg^{2+} substrates.

The high field-strength anionic sites formed by the pore-lining Asp432 side-chains in MgtE have been implicated in facilitating Mg^{2+} selectivity, but the precise mechanism through which selectivity is ultimately achieved remains to be determined. By comparison to other ion channels that harbor key acidic side-chains, it can be suggested that selectivity in MgtE arises through a precise combination of pore dimension and electrostatic potential, and that the conducted substrate is probably a Mg^{2+} ion with its first hydration shell (mostly) intact. It remains a formal possibility that the acidic Asp432 side-chains participate directly in ion coordination in the conductive conformation. In either scenario, considering the overall length observed for the MgtE ion pore, one can assume that it operates in a multi-ion pore configuration.

In CorA, the polar GMN motif at the selectivity filter is known to be capable of coordinating Mg^{2+} ions with their first hydration shells intact. In fact, the CorA pore has been characterized to contain multiple hydrated Mg^{2+} ions bound asymmetrically along its length. Accordingly, we have proposed a knock-on conduction mechanism for CorA in which the outer selectivity filter, central hydrophobic gate, and intracellular electropositive gate are well orchestrated to permit the rapid conduction of hydrated Mg^{2+} substrates. Although one eagerly awaits new structures of MgtE and CorA in their respective open states to examine precisely what chemistries are exposed to the ion conduction pathways, it is fascinating to realize that the problem of selectively transporting Mg^{2+} ions across biological membranes has evolved through (at least) two completely unique structures.

MgtE and CorA share related themes in their Mg^{2+}-based regulation. Conserved acidic residues on intracellular domains from distant regions of the protein are found at domain and subunit interfaces in both channels. In MgtE and CorA, these acidic patches also bind multiple intracellular Mg^{2+} ions. Critically, this common design strategy appears to functionally ensure that all domain motions required for channel activation are tightly sealed and, therefore, highly regulated. As intracellular Mg^{2+} levels decrease, bound ions dissociate, and an ensuing electrostatic repulsion leads to conformational coupling to the pore-lining TM helices. The details here differ, and CorA appears to loose its bound metals and undergo conformational changes sequentially. Nevertheless, MgtE and CorA gating respond to declining intracellular Mg^{2+} levels within a physiologically relevant range, and these findings directly implicate these ion channels in cellular Mg^{2+} sensation, homeostasis and transport. Here, it is important to point out that CorA (or MgtE) can sometimes be the only known Mg^{2+} transport system encoded within a given prokaryotic genome. Thus, while conceptually similar, the unique architectures of MgtE and CorA demonstrate that different regulatory domains can be structurally coupled to gate a Mg^{2+}-selective ion pore. Notably, available data on the related SLC41 and Mrs2–Alr1 proteins indicate that these Mg^{2+} channels also sense and respond to physiologically relevant changes in Mg^{2+} levels within eukaryotic cells [6,59,62,124]. Deciphering the molecular details of these regulation events remains an important challenge for future investigation.

4.2. An emerging prokaryotic cellular Mg^{2+} circuit

A detailed picture of Mg^{2+} homeostasis within prokaryotes has begun to emerge at many levels. CorA was once thought to be constitutively expressed and functionally regulated [91]; but the expression level of CorA at the membrane may actually be more complex [92]. By contrast, the expression of MgtE at the membrane is regulated at the level of transcription [155]. The mRNA encoding *mgtE* contains a riboswitch structure that leads to abortive transcription upon Mg^{2+} binding; so this mRNA effectively functions as a cellular Mg^{2+} sensor to regulate the expression of the ion's transport protein [155]. Remarkably, the mRNA encoding for the MgtA Mg^{2+} transporter is regulated through a similar (yet distinct) riboswitch mechanism [156]. Therefore, in addition to the Mg^{2+}-sensors that are intrinsically built into the regulatory domains of the MgtE and CorA channels, intracellular Mg^{2+}-sensors are also built into the mRNA transcripts that encode these very transporters (at least for *mgtA* and *mgtE*).

On the extracellular side, transcription of the high-affinity MgtA and MgtB Mg^{2+} transporters is initiated by low environmental Mg^{2+} levels through the PhoP–PhoQ two-component signal transduction system [17,156]. Critically, the extracellular Mg^{2+} levels that induce *mgtA* transcription (<100 μM) are below the Mg^{2+} concentrations to which the *mgtE* riboswitch will respond (100–250 μM). Moreover, the trigger for this riboswitch reacts to intracellular Mg^{2+} levels that are set just below those which regulate MgtE and CorA (>250 μM) [39,42,46,47]. This overall organization therefore describes a highly coordinated and interdependent mechanism to sense and respond to extracellular and intracellular Mg^{2+} levels within prokaryotic cells.

In addition to its classical roles as a catalytic and structural co-factor, a global picture of Mg^{2+} homeostasis is emerging whereby the Mg^{2+} ion functions as a key signaling molecule that can (in effect) regulate

its own cellular abundance as well as execute and control discrete genetic cascades. We expect that the growing list of duties known for the MgtE and CorA Mg^{2+} transport systems in microbial physiology (e.g. regulating virulence and protein secretion) will soon supersede their recent structural characterization.

4.3. Implications for understanding eukaryotic Mg^{2+} channels

The available crystal structures and biophysical analysis of MgtE and CorA have set the stage for a better understanding of their eukaryotic counterparts: the SLC41 and Alr1–Mrs2 magnesium channels, respectively. In the SLC41 channel family, functional conservation of essential pore-lining residues immediately suggests a shared TM architecture and conduction mechanism with MgtE. However, since SLC41 channels lack any obvious MgtE-like regulatory domains, unique structural or functional adaptations likely exist. We anticipate that SLC41 channels might be regulated at the level of their TM pore, may engage dedicated regulatory proteins, or can be regulated by posttranslational modifications or subcellular targeting mechanisms [65]. Understanding SLC41 channel regulation and physiology clearly remains an important area of future research.

CorA provides a solid foundation to understand the structure, function, and regulation of its eukaryotic counterparts, including the essential mitochondrial Mg^{2+} channel Mrs2. A very recent crystal structure of the soluble domain of Mrs2 confirms its high structural similarity with CorA [130]; and the essential GMN-selectivity filter motif of Mrs2 also implies a shared mechanism of ion selectivity and conduction [157,158]. Because mitochondria function in a myriad of fundamental physiological processes, we speculate that Mrs2 channel activity is tightly regulated and coupled to the metabolic status of cells through various cellular sensors and signaling pathways. In addition, many eukaryotic CorA family homologues contain significant amino acid extensions beyond their recognizable CorA-like structural domains. Therefore, defining the structure, function and interplay of these auxiliary protein regions in Mrs2 and Alr1 also remains an open area of research in the field.

Future studies of MgtE and CorA will undoubtedly have implications for our understanding of eukaryotic Mg^{2+} channels, but these studies will also have limitations. For example, the MagT1 Mg^{2+} channel required for T cell activation [22] shares absolutely no signature motifs with MgtE or CorA, so drawing analogies appears superfluous at this time. Similarly, the TRPM6 and TRPM7 channels are regulated by the intracellular Mg^{2+} concentration [159] and acidic side-chains have been implicated in divalent cation selectivity [160,161] but these Mg^{2+} channels are more closely related to the tetrameric voltage-gated sodium and calcium channels within their transmembrane domains than either to MgtE or CorA [162,163]. We therefore suspect that crystal structures of a NavAb-like voltage-gated calcium channel [81] will be much more relevant to draw structure–function relationships on the TRPM6 and TRPM7 Mg^{2+} channels. Nevertheless, we are excited about continued and focused structural biology efforts targeting eukaryotic Mg^{2+} transport systems because we truly believe that new structural scaffolds, regulatory mechanisms, and evolutionary relationships are awaiting to be discovered.

5. Figure preparation

Representations of proteins were generated with PYMOL (DeLano Scientific; [164]) for all figures. The solvent accessible pore volume for Figs. 2, 5, and 7 was calculated with MOLE [165].

Acknowledgements

J.P. is grateful to Naomi and Emily Payandeh for their continued support. E.F.P. received support from Canadian Institutes of Health Research (CIHR) Grants MOP-86548 and the Canada Research Chairs Program.

References

[1] M.E. Maguire, J.A. Cowan, Magnesium chemistry and biochemistry, Biometals 15 (2002) 203–210.
[2] M.M. Harding, The geometry of metal–ligand interactions relevant to proteins, Acta Crystallogr. D: Biol. Crystallogr. 55 (1999) 1432–1443.
[3] M.M. Harding, The geometry of metal–ligand interactions relevant to proteins. II. Angles at the metal atom, additional weak metal–donor interactions, Acta Crystallogr. D: Biol. Crystallogr. 56 (2000) 857–867.
[4] M.M. Harding, Metal–ligand geometry relevant to proteins and in proteins: sodium and potassium, Acta Crystallogr. D: Biol. Crystallogr. 58 (2002) 872–874.
[5] R.L. Smith, M.E. Maguire, Microbial magnesium transport: unusual transporters searching for identity, Mol. Microbiol. 28 (1998) 217–226.
[6] G.A. Quamme, Molecular identification of ancient and modern mammalian magnesium transporters, Am. J. Physiol. Cell Physiol. 298 (2010) C407–C429.
[7] D.G. Kehres, M.E. Maguire, Structure, properties and regulation of magnesium transport proteins, Biometals 15 (2002) 261–270.
[8] A. Hartwig, Role of magnesium in genomic stability, Mutat. Res. 475 (2001) 113–121.
[9] W. Yang, J.Y. Lee, M. Nowotny, Making and breaking nucleic acids: two-Mg^{2+}-ion catalysis and substrate specificity, Mol. Cell 22 (2006) 5–13.
[10] M. Selmer, et al., Structure of the 70S ribosome complexed with mRNA and tRNA, Science 313 (2006) 1935–1942.
[11] D.J. Klein, P.B. Moore, T.A. Steitz, The contribution of metal ions to the structural stability of the large ribosomal subunit, RNA 10 (2004) 1366–1379.
[12] G.H. Beaven, J. Parmar, G.B. Nash, B.M. Bennett, W.B. Gratzer, Effect of magnesium ions on red cell membrane properties, J. Membr. Biol. 118 (1990) 251–257.
[13] Z. Grabarek, Insights into modulation of calcium signaling by magnesium in calmodulin, troponin C and related EF-hand proteins, Biochim. Biophys. Acta 1813 (2011) 913–921.
[14] S. Brunet, T. Scheuer, R. Klevit, W.A. Catterall, Modulation of CaV1.2 channels by Mg^{2+} acting at an EF-hand motif in the COOH-terminal domain, J. Gen. Physiol. 126 (2005) 311–323.
[15] G. Mandel, R.H. Goodman, Cell signalling. DREAM on without calcium, Nature 398 (1999) 29–30.
[16] M. Osawa, et al., Mg^{2+} and Ca^{2+} differentially regulate DNA binding and dimerization of DREAM, J. Biol. Chem. 280 (2005) 18008–18014.
[17] E. Garcia Vescovi, F.C. Soncini, E.A. Groisman, Mg^{2+} as an extracellular signal: environmental regulation of *Salmonella* virulence, Cell 84 (1996) 165–174.
[18] I. Gryllos, J.C. Levin, M.R. Wessels, The CsrR/CsrS two-component system of group A *Streptococcus* responds to environmental Mg^{2+}, Proc. Natl. Acad. Sci. U. S. A. 100 (2003) 4227–4232.
[19] S. Derzelle, et al., The PhoP–PhoQ two-component regulatory system of *Photorhabdus luminescens* is essential for virulence in insects, J. Bacteriol. 186 (2004) 1270–1279.
[20] S. Chakraborty, et al., Temperature and Mg^{2+} sensing by a novel PhoP–PhoQ two-component system for regulation of virulence in *Edwardsiella tarda*, J. Biol. Chem. 285 (2010) 38876–38888.
[21] M. Konrad, K.P. Schlingmann, T. Gudermann, Insights into the molecular nature of magnesium homeostasis, Am. J. Physiol. Renal Physiol. 286 (2004) F599–F605.
[22] F. Li, et al., Second messenger role for Mg^{2+} revealed by human T-cell immunodeficiency, Nature 475 (2011) 471–476.
[23] A. Romani, A. Scarpa, Regulation of cell magnesium, Arch. Biochem. Biophys. 298 (1992) 1–12.
[24] H. Rubin, Central role for magnesium in coordinate control of metabolism and growth in animal cells, Proc. Natl. Acad. Sci. U. S. A. 72 (1975) 3551–3555.
[25] R.D. Grubbs, M.E. Maguire, Magnesium as a regulatory cation: criteria and evaluation, Magnesium 6 (1987) 113–127.
[26] V. Trapani, et al., Intracellular magnesium detection: imaging a brighter future, Analyst 135 (2010) 1855–1866.
[27] K.P. Schlingmann, et al., Hypomagnesemia with secondary hypocalcemia is caused by mutations in TRPM6, a new member of the TRPM gene family, Nat. Genet. 31 (2002) 166–170.
[28] R.Y. Walder, et al., Mutation of TRPM6 causes familial hypomagnesemia with secondary hypocalcemia, Nat. Genet. 31 (2002) 171–174.
[29] R.T. Alexander, J.G. Hoenderop, R.J. Bindels, Molecular determinants of magnesium homeostasis: insights from human disease, J. Am. Soc. Nephrol. 19 (2008) 1451–1458.
[30] J.G. Hoenderop, R.J. Bindels, Calciotropic and magnesiotropic TRP channels, Physiology (Bethesda) 23 (2008) 32–40.
[31] S. Silver, Active transport of magnesium in *Escherichia coli*, Proc. Natl. Acad. Sci. U. S. A. 62 (1969) 764–771.
[32] J.E. Lusk, E.P. Kennedy, Magnesium transport in *Escherichia coli*, J. Biol. Chem. 244 (1969) 1653–1655.
[33] S. Silver, D. Clark, Magnesium transport in *Escherichia coli*, J. Biol. Chem. 246 (1971) 569–576.
[34] D.L. Nelson, E.P. Kennedy, Magnesium transport in *Escherichia coli*. Inhibition by cobaltous ion, J. Biol. Chem. 246 (1971) 3042–3049.
[35] M.H. Park, B.B. Wong, J.E. Lusk, Mutants in three genes affecting transport of magnesium in *Escherichia coli*: genetics and physiology, J. Bacteriol. 126 (1976) 1096–1103.
[36] V. Knoop, M. Groth-Malonek, M. Gebert, K. Eifler, K. Weyand, Transport of magnesium and other divalent cations: evolution of the 2-TM-GxN proteins in the MIT superfamily, Mol. Genet. Genomics 274 (2005) 205–216.
[37] D.A. Doyle, et al., The structure of the potassium channel: molecular basis of K^+ conduction and selectivity, Science 280 (1998) 69–77.

[38] M. Hattori, Y. Tanaka, S. Fukai, R. Ishitani, O. Nureki, Crystal structure of the MgtE Mg^{2+} transporter, Nature 448 (2007) 1072–1075.
[39] M. Hattori, et al., Mg^{2+}-dependent gating of bacterial MgtE channel underlies Mg^{2+} homeostasis, EMBO J. 28 (2009) 3602–3612.
[40] V.V. Lunin, et al., Crystal structure of the CorA Mg^{2+} transporter, Nature 440 (2006) 833–837.
[41] S. Eshaghi, et al., Crystal structure of a divalent metal ion transporter CorA at 2.9 Angstrom resolution, Science 313 (2006) 354–357.
[42] J. Payandeh, E.F. Pai, A structural basis for Mg^{2+} homeostasis and the CorA translocation cycle, EMBO J. 25 (2006) 3762–3773.
[43] A. Guskov, N. Nordin, A. Reynaud, H. Engman, A.K. Lundbäck, A.J. Jong, T. Cornvik, T. Phua, S. Eshaghi, Structural insights into the mechanisms of Mg^{2+} uptake, transport, and gating by CorA, Proc. Natl. Acad. Sci. U. S. A. (2012) 18459–18464.
[44] R. Pfoh, A. Li, N. Chakrabarti, J. Payandeh, R. Pomès, E.F. Pai, Structural asymmetry in the magnesium channel CorA points to sequential allosteric regulation, Proc. Natl. Acad. Sci. U. S. A. (2012) 18809–18814.
[45] N. Nordin, A. Guskov, T. Phua, N. Sahaf, Y. Xia, S. Lu, H. Eshaghi, S. Eshaghi, Exploring the structure and function of *Thermotoga maritima* CorA reveals the mechanism of gating and ion selectivity in Co^{2+}/Mg^{2+} transport, Biochem. J. 451 (2013) 365–374.
[46] R. Ishitani, et al., Mg^{2+}-sensing mechanism of Mg^{2+} transporter MgtE probed by molecular dynamics study, Proc. Natl. Acad. Sci. U. S. A. 105 (2008) 15393–15398.
[47] J. Payandeh, et al., Probing structure–function relationships and gating mechanisms in the CorA Mg^{2+} transport system, J. Biol. Chem. 283 (2008) 11721–11733.
[48] J. Hu, M. Sharma, H. Qin, F.P. Gao, T.A. Cross, Ligand binding in the conserved interhelical loop of CorA, a magnesium transporter from *Mycobacterium tuberculosis*, J. Biol. Chem. 284 (2009) 15619–15628.
[49] N. Chakrabarti, C. Neale, J. Payandeh, E.F. Pai, R. Pomes, An iris-like mechanism of pore dilation in the CorA magnesium transport system, Biophys. J. 98 (2010) 784–792.
[50] A.S. Moomaw, M.E. Maguire, Cation selectivity by the CorA Mg^{2+} channel requires a fully hydrated cation, Biochemistry 49 (2010) 5998–6008.
[51] R.L. Smith, L.J. Thompson, M.E. Maguire, Cloning and characterization of MgtE, a putative new class of Mg^{2+} transporter from *Bacillus firmus* OF4, J. Bacteriol. 177 (1995) 1233–1238.
[52] D.E. Townsend, et al., Cloning of the mgtE Mg^{2+} transporter from *Providencia stuartii* and the distribution of mgtE in gram-negative and gram-positive bacteria, J. Bacteriol. 177 (1995) 5350–5354.
[53] L. Aron, C. Toth, H.P. Godfrey, F.C. Cabello, Identification and mapping of a chromosomal gene cluster of *Borrelia burgdorferi* containing genes expressed in vivo, FEMS Microbiol. Lett. 145 (1996) 309–314.
[54] S.K. Tai, G. Wu, S. Yuan, K.C. Li, Genome-wide expression links the electron transfer pathway of *Shewanella oneidensis* to chemotaxis, BMC Genomics 11 (2010) 319.
[55] S. Merino, et al., The MgtE Mg^{2+} transport protein is involved in *Aeromonas hydrophila* adherence, FEMS Microbiol. Lett. 198 (2001) 189–195.
[56] G.G. Anderson, T.L. Yahr, R.R. Lovewell, G.A. O'Toole, The *Pseudomonas aeruginosa* magnesium transporter MgtE inhibits transcription of the type III secretion system, Infect. Immun. 78 (2010) 1239–1249.
[57] A.S. Moomaw, M.E. Maguire, The unique nature of Mg^{2+} channels, Physiology (Bethesda) 23 (2008) 275–285.
[58] A. Goytain, G.A. Quamme, Functional characterization of the mouse [corrected] solute carrier, SLC41A2, Biochem. Biophys. Res. Commun. 330 (2005) 701–705.
[59] A. Goytain, G.A. Quamme, Functional characterization of human SLC41A1, a Mg^{2+} transporter with similarity to prokaryotic MgtE Mg^{2+} transporters, Physiol. Genomics 21 (2005) 337–342.
[60] J. Sahni, B. Nelson, A.M. Scharenberg, SLC41A2 encodes a plasma-membrane Mg^{2+} transporter, Biochem. J. 401 (2007) 505–513.
[61] M. Kolisek, et al., SLC41A1 is a novel mammalian Mg^{2+} carrier, J. Biol. Chem. 283 (2008) 16235–16247.
[62] T. Wabakken, E. Rian, M. Kveine, H.C. Aasheim, The human solute carrier SLC41A1 belongs to a novel eukaryotic subfamily with homology to prokaryotic MgtE Mg^{2+} transporters, Biochem. Biophys. Res. Commun. 306 (2003) 718–724.
[63] Y. Wang, et al., Structure of the formate transporter FocA reveals a pentameric aquaporin-like channel, Nature 462 (2009) 467–472.
[64] R. Dutzler, E.B. Campbell, M. Cadene, B.T. Chait, R. MacKinnon, X-ray structure of a ClC chloride channel at 3.0 A reveals the molecular basis of anion selectivity, Nature 415 (2002) 287–294.
[65] T. Mandt, Y. Song, A.M. Scharenberg, J. Sahni, SLC41A1 Mg^{2+} transport is regulated via Mg^{2+}-dependent endosomal recycling through its N-terminal cytoplasmic domain, Biochem. J. 439 (2011) 129–139.
[66] M. Kolisek, A. Nestler, J. Vormann, M. Schweigel-Röntgen, Human gene SLC41A1 encodes for the Na^{+}/Mg^{2+} exchanger, Am. J. Physiol. Cell Physiol. 302 (2012) C318–C326.
[67] S. Ragumani, J.M. Sauder, S.K. Burley, S. Swaminathan, Structural studies on cytosolic domain of magnesium transporter MgtE from *Enterococcus faecalis*, Proteins 78 (2010) 487–491.
[68] K.P. Locher, Structure and mechanism of ATP-binding cassette transporters, Philos. Trans. R. Soc. Lond. B Biol. Sci. 364 (2009) 239–245.
[69] D.A. Doyle, Structural changes during ion channel gating, Trends Neurosci. 27 (2004) 298–302.
[70] E. Biemans-Oldehinkel, N.A. Mahmood, B. Poolman, A sensor for intracellular ionic strength, Proc. Natl. Acad. Sci. U. S. A. 103 (2006) 10624–10629.
[71] S. Imai, T. Maruyama, M. Osawa, M. Hattori, R. Ishitani, O. Nureki, I. Shimada, Spatial distribution of cytoplasmic domains of the Mg^{2+}-transporter MgtE, in a solution lacking Mg^{2+}, revealed by paramagnetic relaxation enhancement, Biochim. Biophys. Acta 1824 (2012) 1129–1135.
[72] P.J. Stansfeld, M.S. Sansom, Molecular simulation approaches to membrane proteins, Structure 19 (2011) 1562–1572.
[73] E. Vargas, et al., An emerging consensus on voltage-dependent gating from computational modeling and molecular dynamics simulations, J. Gen. Physiol. 140 (2012) 587–594.
[74] D.A. Doyle, Structural themes in ion channels, Eur. Biophys. J. 33 (2004) 175–179.
[75] E.B. Gonzales, T. Kawate, E. Gouaux, Pore architecture and ion sites in acid-sensing ion channels and P2X receptors, Nature 460 (2009) 599–604.
[76] I. Baconguis, E. Gouaux, Structural plasticity and dynamic selectivity of acid-sensing ion channel–spider toxin complexes, Nature 489 (2012) 400–405.
[77] S.H. Heinemann, H. Terlau, W. Stuhmer, K. Imoto, S. Numa, Calcium channel characteristics conferred on the sodium channel by single mutations, Nature 356 (1992) 441–443.
[78] I. Favre, E. Moczydlowski, L. Schild, On the structural basis for ionic selectivity among Na^{+}, K^{+}, and Ca^{2+} in the voltage-gated sodium channel, Biophys. J. 71 (1996) 3110–3125.
[79] J. Yang, P.T. Ellinor, W.A. Sather, J.F. Zhang, R.W. Tsien, Molecular determinants of Ca^{2+} selectivity and ion permeation in L-type Ca^{2+} channels, Nature 366 (1993) 158–161.
[80] P.T. Ellinor, J. Yang, W.A. Sather, J.F. Zhang, R.W. Tsien, Ca^{2+} channel selectivity at a single locus for high-affinity Ca^{2+} interactions, Neuron 15 (1995) 1121–1132.
[81] J. Payandeh, T. Scheuer, N. Zheng, W.A. Catterall, The crystal structure of a voltage-gated sodium channel, Nature 475 (2011) 353–358.
[82] J. Payandeh, T.M. Gamal-El-Din, T. Scheuer, N. Zheng, W.A. Catterall, Crystal structure of a voltage-gated sodium channel in two potentially inactivated states, Nature 486 (2012) 135–139.
[83] X. Zhang, et al., Crystal structure of an orthologue of the NaChBac voltage-gated sodium channel, Nature 486 (2012) 130–134.
[84] L. Yue, B. Navarro, D. Ren, A. Ramos, D.E. Clapham, The cation selectivity filter of the bacterial sodium channel, NaChBac, J. Gen. Physiol. 120 (2002) 845–853.
[85] X. Hou, L. Pedi, M.M. Diver, S.B. Long, Crystal structure of the calcium release-activated calcium channel Orai, Science 338 (2012) 1308–1313.
[86] Y. Zhou, J.H. Morais-Cabral, A. Kaufman, R. MacKinnon, Chemistry of ion coordination and hydration revealed by a K^{+} channel-Fab complex at 2.0 A resolution, Nature 414 (2001) 43–48.
[87] J.H. Morais-Cabral, Y. Zhou, R. MacKinnon, Energetic optimization of ion conduction rate by the K^{+} selectivity filter, Nature 414 (2001) 37–42.
[88] S.P. Hmiel, M.D. Snavely, C.G. Miller, M.E. Maguire, Magnesium transport in *Salmonella typhimurium*: characterization of magnesium influx and cloning of a transport gene, J. Bacteriol. 168 (1986) 1444–1450.
[89] S.P. Hmiel, M.D. Snavely, J.B. Florer, M.E. Maguire, C.G. Miller, Magnesium transport in *Salmonella typhimurium*: genetic characterization and cloning of three magnesium transport loci, J. Bacteriol. 171 (1989) 4742–4751.
[90] M.D. Snavely, J.B. Florer, C.G. Miller, M.E. Maguire, Magnesium transport in *Salmonella typhimurium*: $^{28}Mg^{2+}$ transport by the CorA, MgtA, and MgtB systems, J. Bacteriol. 171 (1989) 4761–4766.
[91] K.M. Papp-Wallace, M.E. Maguire, Regulation of CorA Mg^{2+} channel function affects the virulence of *Salmonella enterica* serovar *typhimurium*, J. Bacteriol. 190 (2008) 6509–6516.
[92] B. Lim, S.H. Sim, M. Sim, K. Kim, C.O. Jeon, Y. Lee, N.C. Ha, K. Lee, RNase III controls the degradation of corA mRNA in *Escherichia coli*, J. Bacteriol. 194 (2012) 2214–2220.
[93] J. Pfeiffer, J. Guhl, B. Waidner, M. Kist, S. Bereswill, Magnesium uptake by CorA is essential for viability of the gastric pathogen *Helicobacter pylori*, Infect. Immun. 70 (2002) 3930–3934.
[94] K.M. Papp-Wallace, et al., The CorA Mg^{2+} channel is required for the virulence of *Salmonella enterica* serovar *typhimurium*, J. Bacteriol. 190 (2008) 6517–6523.
[95] R.L. Smith, M.T. Kaczmarek, L.M. Kucharski, M.E. Maguire, Magnesium transport in *Salmonella typhimurium*: regulation of mgtA and mgtCB during invasion of epithelial and macrophage cells, Microbiology 144 (Pt 7) (1998) 1835–1843.
[96] M.E. Maguire, Hormonal regulation of magnesium uptake: differential coupling of membrane receptors to magnesium uptake, Magnesium 6 (1987) 180–191.
[97] D. Niegowski, S. Eshaghi, The CorA family: structure and function revisited, Cell. Mol. Life Sci. 64 (2007) 2564–2574.
[98] A.J. Worlock, R.L. Smith, ZntB is a novel Zn^{2+} transporter in *Salmonella enterica* serovar *typhimurium*, J. Bacteriol. 184 (2002) 4369–4373.
[99] A.M. Caldwell, R.L. Smith, Membrane topology of the ZntB efflux system of *Salmonella enterica* serovar *Typhimurium*, J. Bacteriol. 185 (2003) 374–376.
[100] Y. Xia, et al., Co^{2+} selectivity of *Thermotoga maritima* CorA and its inability to regulate Mg^{2+} homeostasis present a new class of CorA proteins, J. Biol. Chem. 286 (2011) 16525–16532.
[101] K. Hantke, Ferrous iron uptake by a magnesium transport system is toxic for *Escherichia coli* and *Salmonella typhimurium*, J. Bacteriol. 179 (1997) 6201–6204.
[102] S. Chamnongpol, E.A. Groisman, Mg^{2+} homeostasis and avoidance of metal toxicity, Mol. Microbiol. 44 (2002) 561–571.
[103] J. Sermon, et al., CorA affects tolerance of *Escherichia coli* and *Salmonella enterica* serovar *typhimurium* to the lactoperoxidase enzyme system but not to other forms of oxidative stress, Appl. Environ. Microbiol. 71 (2005) 6515–6523.
[104] V.N. Tripathi, S. Srivastava, Ni^{2+}-uptake in *Pseudomonas putida* strain S4: a possible role of Mg^{2+}-uptake pump, J. Biosci. 31 (2006) 61–67.
[105] D.M. Bui, J. Gregan, E. Jarosch, A. Ragnini, R.J. Schweyen, The bacterial magnesium transporter CorA can functionally substitute for its putative homologue Mrs2p in the yeast inner mitochondrial membrane, J. Biol. Chem. 274 (1999) 20438–20443.
[106] M. Kolisek, et al., Mrs2p is an essential component of the major electrophoretic Mg^{2+} influx system in mitochondria, EMBO J. 22 (2003) 1235–1244.
[107] J. Gregan, et al., The mitochondrial inner membrane protein Lpe10p, a homologue of Mrs2p, is essential for magnesium homeostasis and group II intron splicing in yeast, Mol. Gen. Genet. 264 (2001) 773–781.
[108] G. Sponder, et al., Lpe10p modulates the activity of the Mrs2p-based yeast mitochondrial Mg^{2+} channel, FEBS J. 277 (2010) 3514–3525.

[109] G. Wiesenberger, M. Waldherr, R.J. Schweyen, The nuclear gene MRS2 is essential for the excision of group II introns from yeast mitochondrial transcripts in vivo, J. Biol. Chem. 267 (1992) 6963–6969.
[110] J. Gregan, M. Kolisek, R.J. Schweyen, Mitochondrial Mg^{2+} homeostasis is critical for group II intron splicing in vivo, Genes Dev. 15 (2001) 2229–2237.
[111] M. Piskacek, L. Zotova, G. Zsurka, R.J. Schweyen, Conditional knockdown of hMRS2 results in loss of mitochondrial Mg^{2+} uptake and cell death, J. Cell. Mol. Med. 13 (2009) 693–700.
[112] T. Kuramoto, et al., A mutation in the gene encoding mitochondrial Mg^{2+} channel MRS2 results in demyelination in the rat, PLoS Genet. 7 (2011) e1001262.
[113] M. Kuwamura, et al., Oligodendroglial pathology in the development of myelin breakdown in the dmy mutant rat, Brain Res. 1389 (2011) 161–168.
[114] S. Assou, et al., A gene expression signature shared by human mature oocytes and embryonic stem cells, BMC Genomics 10 (2009) 10.
[115] Y. Chen, et al., Human mitochondrial Mrs2 protein promotes multidrug resistance in gastric cancer cells by regulating p27, cyclin D1 expression and cytochrome C release, Cancer Biol. Ther. 8 (2009) 607–614.
[116] F.I. Wolf, V. Trapani, Multidrug resistance phenotypes and MRS2 mitochondrial magnesium channel: two players from one stemness? Cancer Biol. Ther. 8 (2009) 615–617.
[117] C.W. MacDiarmid, R.C. Gardner, Overexpression of the *Saccharomyces cerevisiae* magnesium transport system confers resistance to aluminum ion, J. Biol. Chem. 273 (1998) 1727–1732.
[118] M.J. Johansson, A. Jacobson, Nonsense-mediated mRNA decay maintains translational fidelity by limiting magnesium uptake, Genes Dev. 24 (2010) 1491–1495.
[119] A. Graschopf, et al., The yeast plasma membrane protein Alr1 controls Mg^{2+} homeostasis and is subject to Mg^{2+}-dependent control of its synthesis and degradation, J. Biol. Chem. 276 (2001) 16216–16222.
[120] G.J. Liu, D.K. Martin, R.C. Gardner, P.R. Ryan, Large Mg^{2+}-dependent currents are associated with the increased expression of ALR1 in *Saccharomyces cerevisiae*, FEMS Microbiol. Lett. 213 (2002) 231–237.
[121] M. Wachek, M.C. Aichinger, J.A. Stadler, R.J. Schweyen, A. Graschopf, Oligomerization of the Mg^{2+}-transport proteins Alr1p and Alr2p in yeast plasma membrane, FEBS J. 273 (2006) 4236–4249.
[122] N.P. Pisat, A. Pandey, C.W. Macdiarmid, MNR2 regulates intracellular magnesium storage in *Saccharomyces cerevisiae*, Genetics 183 (2009) 873–884.
[123] Y. Zhu, A. Davis, B.J. Smith, J. Curtis, E. Handman, *Leishmania major* CorA-like magnesium transporters play a critical role in parasite development and virulence, Int. J. Parasitol. 39 (2009) 713–723.
[124] R. Schindl, J. Weghuber, C. Romanin, R.J. Schweyen, Mrs2p forms a high conductance Mg^{2+} selective channel in mitochondria, Biophys. J. 93 (2007) 3872–3883.
[125] I. Schock, et al., A member of a novel *Arabidopsis thaliana* gene family of candidate Mg^{2+} ion transporters complements a yeast mitochondrial group II intron-splicing mutant, Plant J. 24 (2000) 489–501.
[126] G. Zsurka, J. Gregan, R.J. Schweyen, The human mitochondrial Mrs2 protein functionally substitutes for its yeast homologue, a candidate magnesium transporter, Genomics 72 (2001) 158–168.
[127] C.M. Koth, J. Payandeh, Strategies for the cloning and expression of membrane proteins, Adv. Protein Chem. Struct. Biol. 76 (2009) 43–86.
[128] K. Tan, et al., Structure and electrostatic property of cytoplasmic domain of ZntB transporter, Protein Sci. 18 (2009) 2043–2052.
[129] Q. Wan, et al., X-ray crystallography and isothermal titration calorimetry studies of the *Salmonella* zinc transporter ZntB, Structure 19 (2011) 700–710.
[130] M.B. Khan, B. Sjöblom, R.J. Schweyen, K. Djinović-Carugo, Crystallization and preliminary X-ray diffraction analysis of the N-terminal domain of Mrs2, a magnesium ion transporter from yeast inner mitochondrial membrane, Acta Crystallogr. Sect. F Struct. Biol. Cryst. Commun. 66 (Pt 6) (2010) 658–661.
[131] S.Z. Wang, Y. Chen, Z.H. Sun, Q. Zhou, S.F. Sui, *Escherichia coli* CorA periplasmic domain functions as a homotetramer to bind substrate, J. Biol. Chem. 281 (2006) 26813–26820.
[132] O. Dalmas, et al., Structural dynamics of the magnesium-bound conformation of CorA in a lipid bilayer, Structure 18 (2010) 868–878.
[133] A. Miyazawa, Y. Fujiyoshi, N. Unwin, Structure and gating mechanism of the acetylcholine receptor pore, Nature 423 (2003) 949–955.
[134] R.J. Hilf, R. Dutzler, A prokaryotic perspective on pentameric ligand-gated ion channel structure, Curr. Opin. Struct. Biol. 19 (2009) 418–424.
[135] Y.H. Chen, et al., Homologue structure of the SLAC1 anion channel for closing stomata in leaves, Nature 467 (2010) 1074–1080.
[136] Y. Jiang, et al., Crystal structure and mechanism of a calcium-gated potassium channel, Nature 417 (2002) 515–522.
[137] Y. Wu, Y. Yang, S. Ye, Y. Jiang, Structure of the gating ring from the human large-conductance Ca^{2+}-gated K^{+} channel, Nature 466 (2010) 393–397.
[138] S. Meyer, R. Dutzler, Crystal structure of the cytoplasmic domain of the chloride channel ClC-0, Structure 14 (2006) 299–307.
[139] H. Nury, et al., Crystal structure of the extracellular domain of a bacterial ligand-gated ion channel, J. Mol. Biol. 395 (2010) 1114–1127.
[140] M.A. Warren, et al., The CorA Mg^{2+} transporter is a homotetramer, J. Bacteriol. 186 (2004) 4605–4612.
[141] A.L. Hodgkin, R.D. Keynes, The potassium permeability of a giant nerve fibre, J. Physiol. 128 (1955) 61–88.
[142] B. Hille, Ion Channels of Excitable Membranes, 3rd edition Sinauer Associates, Sunderland MA, 2001.
[143] S. Svidova, G. Sponder, R.J. Schweyen, K. Djinovic-Carugo, Functional analysis of the conserved hydrophobic gate region of the magnesium transporter CorA, Biochim. Biophys. Acta 1808 (2011) 1587–1591.
[144] A. Anishkin, B. Akitake, K. Kamaraju, C.S. Chiang, S. Sukharev, Hydration properties of mechanosensitive channel pores define the energetics of gating, J. Phys. Condens. Matter 22 (2010) 454120.
[145] O. Beckstein, M.S. Sansom, A hydrophobic gate in an ion channel: the closed state of the nicotinic acetylcholine receptor, Phys. Biol. 3 (2006) 147–159.
[146] I. Persson, Hydrated metal ions in aqueous solution: how regular are their structures? Pure Appl. Chem. 82 (2010) 1901–1917.
[147] L.M. Kucharski, W.J. Lubbe, M.E. Maguire, Cation hexaammines are selective and potent inhibitors of the CorA magnesium transport system, J. Biol. Chem. 275 (2000) 16767–16773.
[148] R.E. Hibbs, E. Gouaux, Principles of activation and permeation in an anion-selective Cys-loop receptor, Nature 474 (2011) 54–60.
[149] T. Zhang, Y. Mu, Initial binding of ions to the interhelical loops of divalent ion transporter CorA: replica exchange molecular dynamics simulation study, PLoS One (2012) e43872.
[150] R.L. Smith, E. Gottlieb, L.M. Kucharski, M.E. Maguire, Functional similarity between archaeal and bacterial CorA magnesium transporters, J. Bacteriol. 180 (1998) 2788–2791.
[151] I. Palombo, D.O. Daley, M. Rapp, The periplasmic loop provides stability to the open state of the CorA magnesium channel, J. Biol. Chem. 287 (2012) 27547–27555.
[152] E.M. Froschauer, M. Kolisek, F. Dieterich, M. Schweigel, R.J. Schweyen, Fluorescence measurements of free [Mg^{2+}] by use of mag-fura 2 in *Salmonella enterica*, FEMS Microbiol. Lett. 237 (2004) 49–55.
[153] C. Miller, ClC chloride channels viewed through a transporter lens, Nature 440 (2006) 484–489.
[154] J. Lisal, M. Maduke, The ClC-0 chloride channel is a 'broken' Cl^{-}/H^{+} antiporter, Nat. Struct. Mol. Biol. 15 (2008) 805–810.
[155] C.E. Dann III, et al., Structure and mechanism of a metal-sensing regulatory RNA, Cell 130 (2007) 878–892.
[156] M.J. Cromie, Y. Shi, T. Latifi, E.A. Groisman, An RNA sensor for intracellular Mg^{2+}, Cell 125 (2006) 71–84.
[157] I. Palombo, D.O. Daley, M. Rapp, Why is the GMN motif conserved in the CorA/Mrs2/Alr1 superfamily of magnesium transport proteins? Biochemistry 52 (2013) 4842–4847.
[158] G. Sponder, et al., The G–M–N motif determines ion selectivity in the yeast magnesium channel Mrs2p, Metallomics 5 (2013) 745–752.
[159] L.W. Runnels, TRPM6 and TRPM7: a Mul-TRP-PLIK-cation of channel functions, Curr. Pharm. Biotechnol. 12 (2011) 42–53.
[160] M. Li, et al., Molecular determinants of Mg^{2+} and Ca^{2+} permeability and pH sensitivity in TRPM6 and TRPM7, J. Biol. Chem. 282 (2007) 25817–25830.
[161] M. Mederos y Schnizler, J. Waring, T. Gudermann, V. Chubanov, Evolutionary determinants of divergent calcium selectivity of TRPM channels, FASEB J. 22 (2008) 1540–1551.
[162] V.Y. Moiseenkova-Bell, L.A. Stanciu, I.I. Serysheva, B.J. Tobe, T.G. Wensel, Structure of TRPV1 channel revealed by electron cryomicroscopy, Proc. Natl. Acad. Sci. U. S. A. 105 (2008) 7451–7455.
[163] M. Lichtenegger, T. Stockner, M. Poteser, H. Schleifer, D. Platzer, C. Romanin, K. Groschner, A novel homology model of TRPC3 reveals allosteric coupling between gate and selectivity filter, Cell Calcium (2013), in press.
[164] The PYMOL Molecular Graphics System, vers. 1.5.0.4, Schrödinger, LLC
[165] K. Berka, et al., MOLEonline 2.0: interactive web-based analysis of biomacromolecular channels, Nucleic Acids Res. 40 (2012) W222–W227.